Argininosuccinate Synthase 1 Suppresses Tumor Progression Through Activation of PERK/eIF2α/ATF4/CHOP Axis in Hepatocellular Carcinoma

Sanghwa Kim
Institut Pasteur Korea
Minji Lee
Institut Pasteur Korea
Yeonhwa Song
Institut Pasteur Korea
Su-Yeon Lee
Institut Pasteur Korea
Inhee Choi
Institut Pasteur Korea
I-Seul Park
institut pasteur Korea
jiho Kim
Institut Pasteur Korea
Jin-sun Kim
Asan Medical Center
Kang mo Kim
Asan Medical Center
Haengran Seo (shr1261@ip-korea.org)
Institut Pasteur de Coree

Research

Keywords: Hepatocellular carcinoma (HCC), Argininosuccinate synthase 1(ASS1), endoplasmic reticulum (ER) stress, spheroids, C/EBP Homologous Protein (CHOP)

Posted Date: December 14th, 2020

DOI: https://doi.org/10.21203/rs.3.rs-125320/v1

Version of Record: A version of this preprint was published at Journal of Experimental & Clinical Cancer Research on April 10th, 2021. See the published version at https://doi.org/10.1186/s13046-021-01912-y.

Abstract

Background: Hepatocellular carcinoma (HCC) is one of the most common malignant cancers worldwide, and liver cancer has increased in mortality due to liver cancer because it was detected at an advanced stages in patients with liver dysfunction, making HCC a lethal cancer. Accordingly, we aim to new targets for HCC drug discovery using HCC tumor spheroids.

Methods: Our comparative proteomic analysis of HCC cells grown in culture as monolayers (2D) and spheroids (3D) revealed that argininosuccinate synthase 1 (ASS1) expression was higher in 3D cells than in 2D cells due to upregulated endoplasmic reticulum (ER) stress responses. We investigated the clinical value of ASS1 in Korean patients with HCC. The mechanism underlying ASS1-mediated tumor suppression was investigated in HCC spheroids. ASS1-mediated improvement of chemotherapy efficiency was observed using high content screening in an HCC xenograft mouse model.

Results: Studies of tumor tissue from Korean HCC patients showed that, although ASS1 expression was low in most samples, high levels of ASS1 were associated with favorable overall survival of patients. Here, we found that bidirectional interactions between ASS1 ER stress responses in HCC-derived multicellular tumor spheroids can limit HCC progression. ASS1 overexpression effectively inhibited tumor growth and enhanced the efficacy of in vitro and in vivo anti-HCC combination chemotherapy via activation of the PERK/eIF2α/ATF4/CHOP axis, but was not dependent on the status of p53 and arginine metabolism.

Conclusion: These results demonstrate the critical functional roles for the arginine-metabolism–independent tumor suppressor activity of ASS1 in HCC and suggest that upregulating ASS1 in these tumors is a potential strategy in HCC cells with low ASS1 expression.

Background

Cancers are still the leading cause of human death, and hepatocellular carcinoma (HCC) is one of the most serious forms of cancer. The highest incidence occurs in Eastern Asia and sub-Saharan Africa. Specifically, South Korea ranks highest in the world in liver cancer incidence and mortality rate. Typical first-line therapy for HCC involves surgical resection of the tumor, whereas second-line therapy often includes sorafenib [1], a multi-tyrosine protein kinase inhibitor for treating metastatic or unresectable HCC. However, neither approach is entirely effective against HCC. Therefore, researchers have tried to identify novel target genes and drug candidates for HCC treatment, although none of these developments has yet to significantly improve patient prognoses.

Metabolic alterations in cancer cells are numerous and include aerobic glycolysis, reduced oxidative phosphorylation, and increased generation of biosynthetic intermediates needed for cell growth and proliferation. Recent data have also demonstrated that cancer cells exhibit altered amino acid metabolism [2], and glutamine, serine, glycine, and arginine have been implicated in promoting cancer cell

proliferation [3–5]. In particular, arginine is associated with numerous metabolic pathways pertinent to tumorigenesis, including nitric oxide, creatine, and polyamine synthesis [6, 7].

Several types of tumors have aberrant arginine-metabolic enzymes and rely completely on extracellular arginine to support necessary biological processes, a requirement known as arginine auxotrophy. Many tumors, including HCC, malignant melanoma, malignant pleural mesothelioma, and prostate and renal cancers, are arginine auxotrophic due to their variable loss of argininosuccinate synthase 1 (ASS1), which is severely reduced or absent in numerous types of aggressive and chemoresistant cancers. However, the mechanism of ASS1 downregulation in these tumors has not been fully elucidated in HCC.

The tumor microenvironment (TME) has important physiological roles in cellular differentiation, tumorigenesis, metastasis, and therapeutic efficacy. Presently, two-dimensional (2D) cell-based models fail to predict in vivo efficacy, contributing to limited success in translating new drugs for clinical use. Hence, 2D culture systems alone are not beneficial because the resulting data cannot be utilized for translational research. In contrast, a complex three-dimensional (3D) cell culture system better simulates cellular context and the therapeutically relevant parameters of the in vivo TME, such as pH, oxygen level, metabolite gradients, growth factor penetration, and distribution of proliferating/necrotic cells. In particular, liver cells in a 3D culture system better recapitulate numerous physiological liver functions, including albumin and urea synthesis, bile secretion, and cell polarization.

In our study, we compared the proteomes of HCC cells grown in culture as monolayers (2D) or spheroids (3D) to identify a differential global protein response under these in vitro conditions. ASS1 expression was higher in HCC cells in the 3D culture system than in the 2D system, which illustrates the importance of 3D culture in metabolomics studies and implicates ASS1 as a new target for anti-HCC therapeutics. Moreover, we observed that low ASS1 expression in HCC tissue had a significant effect on the overall survival of patients with liver cancer. We also found that bidirectional interactions between ASS1 and ER stress responses in HCC spheroids modulated HCC cell apoptosis independent of arginine metabolism. Subsequently, we sought to identify compounds that regulate ASS1 expression to improve HCC therapy.

Materials And Methods

Chemical agents

Endoplasmic reticulum stress inducers, including thapsigargin and tunicamycin, cisplatin and the nitric oxide (NO) scavengers such as carboxy-PTIO potassium salt (cPTIO) and Sodium diethyldithiocarbamate trihydrate (Cupral) were purchased from Sigma-Aldrich (St. Louis, MO, USA). The DNA methyltransferase inhibitor; decitabine was purchased from Selleck Chemicals (Houston, TX, USA).

Cell lines and cultures

The HCC cell lines SNU449, SNU475, SNU398, SNU898, Huh7, HepG2, Hep3B and PLC/PRF/5 were purchased from the Korean Cell Line Bank. Huh6 cells were kindly provided by Dr. Ralf Bartenschlager

(University of Heidelberg, Germany). All HCC cells were maintained in RPMI (Welgene, Korea) or Dulbecco's Modified Eagle Medium (DMEM; Welgene, Korea) containing 10% fetal bovine serum (FBS; Gibco, Grand Island, NY, USA) and 1% penicillin/streptomycin solution (p/s; Gibco, Grand Island, NY, USA). Fa2N-4, a human immortalized hepatocyte cell line, was obtained from Xenotech (Lenexa, KS, USA) and first cultured in serum-containing plating medium (K4000; Xenotech). Miha. Cells were kindly provided by Dr. Kim. K. M from Asan medical. To produce tumor spheroids, HCC cells seeded at a density of 6×10^3 cells/well in 96-well round-bottom ULA microplates (Corning Life Sciences, Corning, NY, USA). All cells were maintained in a 5% CO2 humidified incubator at 37 °C.

Ethics approval and patient consent

This study was conducted in accordance with the Declaration of Helsinki, and samples were provided from patients of ASAN medical center. Approximately 60 patients with a diagnosis of liver cancer who were treated and followed up in the clinic participated. The study was approved by the Human Research Ethic Committee of ASAN medical center (Permit Number: 2007 – 0332). The Institutional Review Board of ASAN medical center complies with the related laws including ICH, KGCP, and the Bioethics and Safety Act of Korea. Written informed consent for the use of tissues for research purposes was obtained from patients at the time of tumor specimen procurement.

Primary culture of HCC-derived cells

We acquired a portion of human HCC tumors immediately after surgical resection. The tumors were immersed in Hanks' balanced salt solution (Gibco-ThermoFisher, Waltham, MA, USA). Patient-derived primary HCC cell lines (17S-35372B, 17S-64007, 17S-68354, 17S-21612B, 27273, 101509, 103201, and 116261) were generated from liver cancer tissues of eight Korean patients.

Proteomic analysis

Monolayer (2D) and tumor spheroid (3D) lysates from patient-derived primary cells were separated and analyzed using nanoACQUITY UPLC system (Waters, Milford, MA, USA) directly coupled to a Finnigan LCQ DECA ion trap mass spectrometer (Thermo Fisher). The samples were analyzed using a MS/MS spectra system (Thermo Quest, San Jose, CA, USA) and processed using SEQUEST software purchased from Thermo Fisher.

Microarray and bioinformatics analysis

From the generated microarray data, we selected genes identified by FUNRICH (functional enrichment analysis tool; http://www.funrich.org) and REACTOME database pathway whose expression levels changed ≥ 2-fold (absolute) when enriched by ASS1-overexpressing HCC spheroids. We then determined if these genes were enriched or depleted in molecular functions, physiological processes, and biological pathways.

Western blot assay

Cells from resected tumors were lysed by RIPA buffer (CureBio, Seoul, Korea) for 30 min at 4 °C, and lysates were collected by centrifugation at 20,000 g for 30 min. The protein concentration of each group's cell lysate was measured using the Pierce™ BCA protein Assay Kit (ThermoFisher, Cambridge, MA, USA). Equal amounts of proteins were separated on an SDS-PAGE gel using the electrophoretic technique. The gel was transferred to a nitrocellulose membrane using a BioRad transfer system (Hercules, CA, USA) and blocked with 5% skim milk. Primary antibodies for hybridization included those for ATF6, IRE1α, ATF3, GRP78, cleaved caspase 3, PARP, Snail-1 (all from Cell Signaling Technology, Danvers, MA, USA), ASS1, CHOP, XBP1, α-SMA, N-cadherin, E-cadherin (all from Abcam, Cambridge, UK), and β-actin (Sigma-Aldrich, St Louis, MO, USA). Secondary antibodies conjugated with horseradish peroxidase were then applied to the blots. Resulting protein bands were detected using the LuminoGraph II system (ATTO, Tokyo, Japan).

Immunoprecipitation (IP) analysis

The cell lysates were harvested and lysed with lysis buffer containing protease inhibitors. The cell extracts (2 mg/500 µl) were conducted immunoprecipitation using Pierce™ Co-immunoprecipitation Kit (Thermo Fisher, Cambridge, MA, USA) following to manufacturer`s instructions. The samples were incubated with anti-Flag (Thermo Fisher) at 4 °C overnight, and conducted by western blot assay.

Immunofluorescence (IF)

For immunofluorescence, the samples were fixed in 4% paraformaldehyde (PFA) and washed in DPBS with Tween 20 (DPBS-T). After than the samples were blocked in DPBS-T plus 10% NGS for 1 h at room temperature. Samples were then incubated with primary antibodies and secondary fluorophore-conjugated antibodies. Cell nuclei were stained using Hoechst 33342 (1:1000, MOP-H3570; ThermoFisher, Cambridge, MA, USA). After washing, the samples were mounted, and fluorescence images were detected using an automated high-content imaging system (OPERETTA, PerkinElmer, Waltham, MA, USA) and confocal laser scanning microscope (CLSM II; LSM710A, Carl Zeiss, Germany). The results were analyzed by an in-house software tool and HARMONY 3.5.1. (PerkinElmer, Waltham, MA, USA)

Transfection with siRNAs

Huh7 cells were transfected with 500 nM siRNA/5 × 105 cells using the Lipofectamine2000® transfection reagent (ThermoFisher, Cambridge, MA, USA). siRNA targeting ASS1 were purchased from Dharmacon (Lafayette, CO, USA; L-004819-00-0005, SMARTpool:ON-TARGETplus ASS1 siRNA, USA), Bioneer (Daejeon, Korea; siRNA ID:445-1, 445-2 and 445-3) and Santa Cruz Biotechnology (sc-45810, Santa Cruz Biotechnology Inc., Dallus, TX, USA). siRNA targeting CHOP were purchased from Dharmacon (Lafayette, CO, USA; L-010257-00-0005, SMARTpool:ON-TARGETplus CHOP siRNA, Lafayette, CO, USA) siRNAs were transfected into ASS1-overexpressing Huh7 cells using Lipofectamine RNAiMAX (Invitrogen, Carlsbad, CA, USA) reagent with Opti-MEM, and the cells were incubated in 37 °C for 48 h.

Cell survival and apoptosis analysis assay

To measure the cell viability, ATP level was analyzed using the CellTiter-Glo luminescent cell viability assay kit (Promega, Madison WI, USA). To analyze apoptosis capacity, Caspase3/7 activity and Annexin V activity were measured using the Caspase-Glo 3/7 assay kit (Promega, Madison, WI, USA) and Real-time-Glo™ Annexin V Apoptosis Assay kit (Promega, Madison, WI, USA) following manufacturer`s instructions.

Wound healing and colony formation assays

Transfected pCMV3 or ASS1-Flag (overexpression) Huh7 cells were seeded at 1×10^6 in RPMI with 10% FBS in 6-well plates. After 24 h, cells were grown to full confluence in plates and scratched using a pipette tip. Cells were washed with PBS to remove cellular debris and allowed to migrate for 24 h. Cell migration images were captured using light microscopy, and five fields in the wounded areas were noted. For colony formation assays, 1×10^3 transfected pCMV3 or ASS1-Flag Huh7, SNU475, and SNU449 cells were transferred to 6-well plates. Starting the day after seeding, the medium was replaced every 3 days. The cells were cultured for 14 days, and then the plates were washed with Dulbecco's PBS (DPBS) and stained with crystal violet (Sigma-Aldrich, St Louis, MO, USA). The number of colonies were counted and analyzed.

Dose-response curve experiments

Huh7, SNU475 and Hep3B cells transfected with pCMW3, ASS1-Flag, or siRNA (ASS1) were seeded in 384-well plates at a density of 2×10^3 cells/well. For single treatment, the concentration of compounds including cisplatin, thapsigargin, and NO scavengers (cPTIO and cupral) was diluted from 10 μM to 39.06 nM in 0.5% DMSO (v/v). After 48 h, the cells were fixed in 4% paraformaldehyde (PFA) for 10 min and washed twice with Dulbecco's PBS (DPBS). Cell nuclei were stained using Hoechst 33342. To detect an enough cells using an automated high-content imaging system (OPERETTA, PerkinElmer, Waltham, MA, USA), five field images were captured and collected from each well. The images were analyzed by an in-house software tool and HARMONY 3.5.1. (PerkinElmer, Waltham, MA, USA).

Luciferase assay

To construct an ASS1-Gluc stable cell line, HEK293 cells were transfected with the ASS1 promoter and firefly luciferase gene sequence in the pEZX-PG02.1 lentiviral vector. Transduced cells were selected using puromycin. After constructing the stable cell line, cells were seeded onto 96-well plates. The luciferase reporter assay was conducted with the Nano-Glo® Luciferase Assay System (Promega, Madison, WI, USA) according to the manufacturer's instructions. The luminescence from firefly and Renilla luciferase were measured by a luminometer (Berthold, Bad Wildbad, and Germany).

Xenograft mouse model

Huh7 cells (5×10^6 cells/mouse) were transplanted following resuspension with Matrigel (reduced matrix growth factor reduced; BD Biosciences) and orthotopically injected into 5-week-old male BALB/c nude mice (Central Lab. Animal, Inc., Seoul, Korea). The mice kept in a laboratory animal facility with a constant temperature of 20 °C ± 2 °C and relative humidity of 50% ± 10% under regular light-dark cycle. At

2 weeks post-injection, the mice were randomly divided into 6 groups (5 mice per group): 1) control (saline), 2) cisplatin 5 mpk (mg/kg body weight), 3) decitabine 1 mpk, 4) decitabine 2 mpk, and combination groups including 5) cisplatin 5 mpk + decitabine 1 mpk and 6) cisplatin 5 mpk + decitabine 2 mpk. Each compound or combination was then administered for 1 week by I.P. injection, after which the mice were sacrificed. Throughout the experimental period, body weight and tumor size were measured twice a week using calipers and calculated tumor volume (mm^3) by the standard formula. The experiment was approved by the Institutional Animal Care and Use Committee (IACUC) of ASAN medical center.

Statistical analysis

The statistical significance between groups was determined using the Student's t-test with a Newman-Keuls post-hoc test using Prism 5 (GraphPad, San Diego, CA, USA). $P < 0.05$ was considered statistically significant.

Results

The expression of ASS1 is upregulated in HCC spheroids

In order to investigate the role of cell adhesion, mediated by cell-cell and cell-ECM interactions in the tumor microenvironment, in the molecular mechanism underlying ASS1 function, we compared the proteomes of HCC cells cultured as monolayers (2D) or spheroids (3D) to identify a global protein response in the different *in vitro* conditions [Figure 1-A]. We focused on polypeptides upregulated by at least 4-fold in HCC spheroids relative to monolayers ($P \leq 0.05$). Specifically, six proteins (nucleophosmin, peroxiredoxin, HSF5, aldolase A, HSPD1, and ASS1) were expressed at a higher level in HCC cell spheroids than in monolayers [Figure 1-B]. Thus, we investigated the expression patterns of these proteins in HCC monolayers and spheroids.

Western blot analysis revealed that aldolase A, HSPD1, and ASS1, but not nucleophosmin and peroxiredoxin, were significantly increased in HCC spheroids compared to monolayers. HSF5 was not detected by western blotting in HCC monolayers or tumor spheroids [Supplementary Fig. 1 and Fig. 1-C]. Because metabolic alterations have been highlighted recently as targets for HCC therapy, we focused on the metabolism-related protein ASS1 among HCC spheroid-specific proteins.

To confirm whether ASS1 expression is cell adhesion status - dependent, we measured ASS1 protein expression in lysates of monolayers and spheroids of HCC cell lines Huh7, Hep3B, SNU475 and SNU449 and of Fa2N-4 normal hepatocytes. In the monolayer culture system, the HCC cell lines scarcely expressed ASS1, whereas Fa2N-4 cells showed higher ASS1 expression. Interestingly, ASS1, which was minimally expressed in HCC monolayers, was highly expressed in HCC spheroids [Figure 1-C] and *ASS1* mRNA expression was also altered in a culture-type–dependent manner [Figure 1-D].

To avoid using the less physiologically relevant genetically defined human cell lines, we attempted to confirm increased ASS1 expression in spheroids cultured using primary HCC cells isolated from liver resection specimens of five patients. We measured ASS1 mRNA and protein in lysates of monolayers and spheroids cultured from patient-derived primary HCC cells. Similar to the results with HCC cell lines, ASS1 mRNA and protein were expressed at higher levels in patient-derived HCC spheroids than in monolayers [Figure 1-E, F]. These results suggested that ASS1 expression is upregulated in the 3D HCC tumor microenvironment.

HCC patients expressing higher levels of ASS1 have a more favorable prognosis

Epigenetic silencing via methylation of the *ASS1* promoter was previously demonstrated in certain cancer types, so we assessed *ASS1* mRNA levels in immortalized normal hepatocyte (Fa2N-4 and Miha cell) spheroids and in HCC spheroids derived from Asian (SUN449, SUN475, SNU878, and SNU398 cells) and Caucasian (Hep3B, Huh6, HepG2, and PLC/PRF/5 cells) patients. Reverse transcription (RT)-quantitative (q) PCR analyses showed that all HCC spheroids express lower levels of ASS1 than spheroids of normal hepatocytes [Figure 2-A]. Next, we also examined ASS1 protein expression in HCC spheroids derived from Asian and Caucasian HCC patients. All spheroids of Korean patient-derived HCC cells showed dramatically lower ASS1 expression than spheroids of normal hepatocytes. In contrast, some spheroids of Caucasian patient-derived liver cancer lines, such as Hep3B and PLC/PRF/5, exhibited ASS1 expression similar to that of normal hepatocyte spheroids. The ASS1 expression appears to be lower in HCC cells derived from Asian patients than from Caucasian patients [Figure 2-B].

We investigated *ASS1* mRNA expression in tumor spheroids from primary HCC cells derived from eight Korean liver cancer patients. The cells were passaged only 3–6 times. We also measured *ASS1* mRNA expression in tumor spheroids from six Asian patient-derived HCC lines (SUN449, SUN475, SNU878, AMC-H1, AMC-H2, and Huh7), three Caucasian patient-derived liver cancer lines (Hep3B, Huh6, and adenocarcinoma line SK-Hep1), and normal hepatocytes (Fa2N-4). All tumor spheroids of the eight Korean patients displayed significantly lower *ASS1* mRNA expression than in spheroids of normal hepatocytes. Expression of *ASS1* mRNA was also lower in HCC spheroids of Caucasian and Asian patients than in spheroids of normal hepatocytes [Figure 2-C].

Based on these results, we next investigated the clinical significance of ASS1 expression in Korean patients with liver cancer because its incidence and mortality rate is the highest in the world, even though ASS1 is not prognostic in liver cancer, according to The Cancer Genome Atlas (TCGA) program.

ASS1 expression was quantified by western blotting in tissue from 58 Korean patients with nodular liver cancer and hepatitis B infection. Representative ASS1 expression patterns are shown in Fig. 2-D and Supplementary Fig. 2.

Because ASS1 expression varied among patients, we performed further statistical analysis. The 58 liver cancer patients were divided into three groups based on the results of western analysis: 1) higher ASS1

expression in tumor vs. peritumoral tissue (n = 7); 2) lower ASS1 expression in tumor vs. peritumoral tissue (n = 51); and 3) no significant difference in ASS1 expression between tumor and nontumor tissue (n = 0). The results of this analysis indicated that ASS1 expression was lower in tumor tissue than peritumoral tissue from Korean HCC patients. We wondered whether a correlation existed between ASS1 expression in tumor tissue and survival rate after resection in patients with liver cancer. The two groups with differential ASS1 expression exhibited significant differences in 10-year survival rates after resection that were significantly higher when ASS1 expression was higher in tumor vs. peritumoral tissues [Figure 2-E].

These results suggest that HCC patients with increased ASS1 expression in tumor tissue have a more favorable prognosis than patients with lower ASS1 expression, which prompted us to focus on the potential tumor suppressor roles of ASS1 during HCC progression.

ASS overexpression inhibits HCC tumor growth and improves chemotherapy efficacy

To investigate the effects of altered ASS1 expression on HCC cell growth and migration, we established ASS1-overexpressing HCC cell lines. First, we examined whether ASS1 controlled cell growth in HCC. Cell survival was diminished by ASS1 overexpression in Huh7 and SNU475 cells [Figure 3-A], whereas the cell doubling times increased in Huh7, SNU475 and SNU449 cells [Figure 3-B].

To determine whether the ASS1-induced inhibition of cell growth was associated with an increase in apoptosis, we evaluated apoptosis-related parameters using Annexin V-FITC/PI assay kit. Following ASS1 overexpression, the number of Annexin V-positive Huh7 and SNU475 cells was increased [Figure 3-C]. Additionally, we measured caspase-3/7 activity and expression of cleaved poly (ADP-ribose) polymerase (PARP) in ASS1-overexpressing HCCs. ASS1 overexpression not only promoted caspase-3/7 activity [Figure 3-D], but also increased levels of cleaved PARP in Huh7 and SNU475 cells [Figure 3-E]. These results showed that ASS1 overexpression can inhibit HCC growth by delaying cell growth and inducing apoptosis.

Wound-healing assays revealed that the migratory capacity of HCC cells was attenuated by ASS1 expression [Figure 3-F]. Because cells in epithelial-to-mesenchymal transition (EMT) acquire increased migratory capacity, we next measured the expression of EMT-related proteins (E-cadherin, N-cadherin, α-SMA, and Snail-1) in ASS1-overexpressing HCC cells. Although upregulation of N-cadherin, Snail-1, and α-SMA and downregulation of E-cadherin enhance EMT, which plays a pivotal role during HCC progression, EMT was inhibited by ASS1 overexpression in Huh7 and SNU475 cells [Figure 3-G].

Previous reports showed that cisplatin sensitivity is restricted during cancer in an ASS1- expression–dependent manner. Herein, we observed responses to cisplatin with respect to ASS1 expression levels in Hep3B and PLC/PRF/5 cells, which normally express higher than average levels of ASS1 among HCC cell lines, and Huh7 and SNU475 cells, which minimally express ASS1. When we compared the sensitivities of normal and ASS1-deficient Hep3B cells to cisplatin treatment coupled with siRNA-mediated ASS1

knockdown, depletion of ASS1 shifted the cisplatin IC_{50} from 4.231 μM to 9.372 μM [Figure 3-H]. Moreover, ASS1-deficient PLC/PRF/5 cells showed slight resistance to cisplatin relative to control-siRNA-transfected cells [Supplementary Table II], whereas ASS1-overexpressing Huh7 and SNU475 cells displayed greater sensitivity to cisplatin than wild-type cells [Figure 3-I, Supplementary Table III]. Furthermore, sensitivity to sorafenib, which is the only systemic chemotherapeutic agent available for HCC, was slightly affected by altered ASS1 expression [Supplementary Table II, III].

ASS1 is upregulated through ER stress responses in HCC spheroids

To identify genes associated with ASS1 upregulation, we performed microarray analysis using ASS1-overexpressing HCC spheroids. Four genes, *ASNS*, *ATF3*, *CHOP*, and *HSPA1A*, were selected because their expression levels changed ≥ 2-fold with ASS1 overexpression in HCC cells. Based on the results of pathway analysis *ATF4*, *ATF6*, *HSP90B1*, *HSPA5*, *CALR*, and *XBP1* were also examined for their roles in ASS1 signaling [Figure 4-A, Supplementary Table I].

Because most of the genes selected from the microarray analysis were closely related to potential ER stress responses, and the mechanism of ASS1 overexpression in spheroids was unknown, we explored the possible correlation between ER stress response and ASS1 expression in HCC monolayers or HCC spheroids. As expected, HCC spheroids of SNU475, SNU449, and Huh7 cells exhibited higher expression levels of ER stress-response–related proteins (CHOP, XBP1, GRP78, and ATF3) and ASS1 than monolayer cells [Figure 4-B].

To determine whether ER stress contributes to ASS1 synthesis in HCC microenvironments, we analyzed the effects of thapsigargin and tunicamycin, which induce ER stress and the unfolded protein response (UPR), on regulation of ASS1 expression in Huh7 and SNU475 cells. *ASS1* mRNA expression significantly increased in a dose-dependent manner with thapsigargin [Figure 4-C] and tunicamycin [Figure 4-D] treatment in Huh7 cells and SNU475 cells by enhancing ASS1 promoter activity [Figure 4-E, F]. Accordingly, treatment with thapsigargin and tunicamycin resulted in increasing ASS1 protein expression in Huh7 and SNU475 cells [Figure 4-G, H]. Furthermore, immunohistochemistry results revealed that ASS1 is translocated from the cytoplasm to the ER during thapsigargin- or tunicamycin-induced ER stress response and UPR in HCC cells [Figure 4-I]. These results suggested that ASS1 is upregulated via ER stress response in the HCC microenvironment.

ASS1 controls cell fate through upregulation of PERK/eIF2α/ATF4/CHOP signaling in HCC

We next focused on the functional roles of ASS1 with respect to ER stress response in HCC. Among three ER stress sensor proteins, inositol-requiring enzyme-1 (IRE1), PKR-like ER kinase (PERK), and activating transcription factor-6 (ATF6), ASS1 overexpression in Huh7 and SNU475 cells led to notable upregulation of PERK and ATF6 expression. The PERK/eIF2α/ATF4/CHOP pathway has pivotal roles in the induction of apoptotic cell death during ER stress responses [8]. ATF6 is cleaved by S1P and S2P proteases in the

Golgi apparatus under ER stress conditions, and then cleavage of ATF6 (p50 ATF6f) leads to upregulation of chaperones, XBP1, and the pro-apoptotic factor CHOP via translocation to the nucleus [9]. Cancer cells exploit the IRE1α-XBP1s arm of the ER stress response to efficiently adjust their protein-folding capacity and ensure survival under hostile tumor microenvironmental conditions [10]. Interestingly, ASS1 overexpression increased expression of proteins in PERK/eIF2α/ATF4/CHOP signaling nodes and expression of XBP1u, which is induced by ATF6, whereas expression of proteins in the IRE1α-XBP1s pathway was not altered in HCCs by ASS1 overexpression.

CHOP (DDIT3) in the PERK/eIF2α/ATF4/CHOP pathway, also known as C/EBP homologous protein and DNA damage inducible transcript 3, plays a central role in ER stress-mediated apoptosis [11–13].

Because its expression was substantially increased in ASS1-overexpressing HCC cells, we explored whether ASS1 overexpression could increase ER stress-mediated apoptosis. Following treatment of SNU475 and Huh7 cells with thapsigargin for 48 h, markers of apoptosis, such as cleaved PARP and cleaved caspase-3, as well as CHOP, were significantly upregulated in ASS1-overexpressing vs. wild-type SNU475 and Huh7 cells [Figure 5-B]. ASS1-overexpressing SNU475 cells displayed greater sensitivity to thapsigargin than wild-type SNU475 cells [Figure 5-C]. ASS1 was also silenced in Hep3B cells to confirm whether ASS1 knockdown would inhibit ER stress-mediated apoptosis in HCC cells that innately express higher than average levels of ASS1. Compared with control- siRNA-transfected cells, ASS1 knockdown led to significantly reduced survival of cells treated with thapsigargin [Figure 5-D]. These results demonstrated that ASS1 overexpression could facilitate and magnify ER stress-mediated apoptosis in HCC.

Because ASS1 overexpression concurrently elevated CHOP levels and facilitated ER stress-mediated apoptosis, we next examined whether CHOP is the key mediator of the ASS1-mediated apoptosis in HCCs.

Rescue experiments downregulating CHOP in ASS1-overexpressing HCC cells were performed using a colony-forming assay. Inhibition of CHOP restored diminished clonogenic survival by ASS1 overexpression in Huh7 and SNU475 cells [Figure 5-E]. Moreover, increased levels of cleaved PARP and cleaved caspase-3 by ASS1 overexpression were also inhibited by depletion of CHOP in HCCs [Figure 5-F]. These results demonstrate that CHOP is the key mediator of ASS1-mediated apoptosis in HCCs.

We next examined whether ASS1 directly modulates CHOP expression using siRNAs targeting ASS1 in ASS1-ovexpressing Huh7 cells. Transfection with siRNA targeting ASS1 effectively attenuated expression of CHOP [Figure 5-G]. To explore the relationship between ASS1 and CHOP *in vivo*, we investigated expression patterns of ASS1 and CHOP in patient HCC tissue. ASS1 protein expression was proportionally correlated with CHOP expression [Figure 5-H]. The patterns of ASS1 and CHOP expression revealed by immunostaining of HCC tissue showed that the expression levels of those two proteins were not only correlated with one another but that the proteins were also co-localized [Figure 5-I]. Taking a closer look, co-localization of ASS1 and CHOP was also observed in HCC cells [Figure 5-J]. To evaluate the direct interaction between ASS1 and PERK pathway related genes including PERK, ATF4 and CHOP in

response induction of ER stress, we conducted immunoprecipitation (IP) assay with anti-flag in ASS1-flag overexpressed cells. As the result, ATF4 and CHOP were dominantly interacted with ASS1, especially in response ER stress induce condition [Figure 5-K].

ASS1 acquires tumor suppressor activity independent of arginine metabolism and the p53 pathway

Through arginine synthesis, ASS1 plays critical key roles in the production of nitric oxide (NO), which paradoxically exhibits both cancer-promoting and -restricting effects depending on the cellular environment. Thus, we also explored whether the effects of ASS1 on ER stress-mediated apoptosis is dependent on NO production in HCC and found that NO was increased in ASS1-overexpressing cells and was reduced in ASS1-depleted cells [Figure 6-A]. We detected altered expression of CHOP in ASS1-overexpressing cells following treatment with the NO scavengers cPTIO and cupral. Increased levels of CHOP previously detected in ASS1-overexpressing HCC cells were not altered by NO scavenging [Figure 6-B]. Moreover, treatment with cPTIO and cupral did not affect inhibition of cell survival caused by ASS1 overexpression [Figure 6-C]. These results indicate that ER stress-mediated apoptosis in ASS1-overexpressing cells is not related to NO production derived from arginine metabolism.

As *p53* is a well-characterized tumor suppressor gene, we determined whether ASS1-associated ER stress could regulate the p53 pathway in HCCs. ASS1 overexpression did not alter *p53* or *p21* expression in p53 wild-type HCC (Fa2N-4 and HepG2) cells, as well as CHOP and phospho-histone H2AX (γ-H2AX) expression also did not change by ASS1 expression in p53 wild-type HCC cells [Figure 6-D]. In addition, cell survival by ASS1 expression was not distinctly observed in p53 wild-type cells [Figure 6-E]. However, expression of CHOP and γ-H2AX were dramatically increased by ASS1 overexpression exclusively in p53-mutant HCC (Huh7, SNU475, and Hep3B) cells [Figure 6-F]. Moreover, clonogenic survival by ASS1 expression were significantly diminished in p53-mutant HCC cells [Figure 6-G]. These results demonstrate that the ASS1-dependent DNA damage and -CHOP associated apoptosis are more facilitated in p53-mutant HCC than in p53 wild-type HCC cells.

Decitabine improves the efficacy of anti-HCC chemotherapeutic drugs by increasing ASS1 expression

Because ASS1 plays a key role in ER stress-mediated apoptosis, we aimed to identify modulators of ASS1 expression to improve HCC therapy. Hence, we performed screening to identify compounds that specifically alter the activity of the *ASS1* promoter.

We screened 3,527 compounds selected from compound libraries (including LOPAC, Selleck anticancer and kinase inhibitors, FDA collection, and IND drugs) for drug repositioning in duplicate to confirm the reproducibility of observed effects. Compounds were screened at an initial concentration of 1 uM with a readout looking at an increase in ASS1 promoter activity. Positive and negative controls would be 10 nM thapsigargin and 0.01% dimethyl sulfoxide. A Pearson correlation coefficient of 0.71 for replicate screens indicated that the assay was reliable [Figure 7-A]. Fifteen compounds, including thapsigargin, constituted

the primary hits that significantly elevated *ASS1* promoter activity [Supplementary Table IV]. Through follow-up dose-response studies performed to quantify the potency of selected hits [Supplementary Fig. 3], we found that decitabine, a hypomethylating agent, most efficiently elevated *ASS1* promoter activity among the hits in HCC cells [Figure 7-B], although treatment with decitabine did not result in anti-HCC efficacy [Supplementary Fig. 4].

Furthermore, expression of both ASS1 and CHOP was significantly enhanced in the presence of decitabine in Huh7, SNU449, and SNU475 cells [Figure 7-C].

Next, we investigated whether increasing ASS1 expression via decitabine treatment improved efficacy of conventional chemotherapy against HCC. Treatment with decitabine significantly enhanced sensitivity to cisplatin in Huh7 [Figure 7-D, E] and SNU449 cells [Figure 7-F]. Expression of apoptosis markers, such as cleaved PARP and caspase-3, was increased in HCC cells after treatment with cisplatin and decitabine in Huh7 and SNU 475 cells [Figure 7-G].

To determine whether decitabine could enhance the efficacy of anti-HCC therapies *in vivo*, we transplanted Huh7 cells into BALB/c mice. Administration of decitabine or cisplatin alone led to a subtle reduction of tumor growth or tumor regression, respectively. However, combination treatment with both agents significantly reduced tumor volume vs. treatment with cisplatin alone [Figure 8-A, B], suggesting that decitabine can act as a therapeutic adjuvant with cisplatin to treat HCC. Western analysis of tumor tissue showed that treatment with cisplatin plus decitabine increased levels of cleaved PARP relative to cisplatin alone [Figure 8-C, D] and administration of decitabine induced upregulation of ASS1 in HCC-implanted xenograft mice, as *in vitro* [Figure 8-C, E]. These data suggest that decitabine might serve as a sensitizer for highly efficient treatment of HCC with cisplatin.

Taken together, our results show that treatment with decitabine increases ASS1 expression, thereby facilitating the robust therapeutic activity of combined decitabine and anti-HCC therapies, such as cisplatin.

Discussion

HCC is the most common primary malignancy of the liver and progresses rapidly, leading to poor overall survival and, consequently, short treatment duration. Despite high-profile failures of multiple VEGFR-targeting agents against HCC, substantial research and development efforts continue in this area [14–17]. For example, sorafenib, a multi-kinase inhibitor, was approved for treating advanced HCC in 2007, [18], but its effectiveness and safety have not been extensively demonstrated [19]. Moreover, HCC rapidly becomes sorafenib-resistant [20]. Nevertheless, lenvatinib [21], regorafenib [22], ramucirumab [23] and cabozantinib [24], which recapitulate the mechanisms of sorafenib as VEGFR inhibitors, are expected to be approved for second-line treatment of advanced HCC in the United States and EU5, but not in the Asia-Pacific region. Unfortunately, the majority of HCC cases occur in this region, which highlights the serious challenge of HCC drug discovery, as clinical trials do not accurately reflect the epidemiology of this disease.

To supplement the development of VEGF/VEGFR inhibitors for HCC therapy, new targets are currently being investigated, such as PD-1/PD-L1 [25, 26], CTLA-4[27, 28], c-Met[29], TGF[30], PI3K/PTEN/Akt/mTOR[31], and Hedgehog [32]*etc*. Additionally, dysregulation of many signaling pathways has been linked to HCC development and progression, so researchers have sought to derive novel target genes and drug candidates related to these pathways. Recently, metabolic reprogramming of the tumor microenvironment through alterations in intracellular and extracellular metabolites and metabolic pathways have also been considered valuable targets for HCC therapy. Most tumor cells must adapt their metabolism to survive and proliferate in this dynamic and often harsh TME [33, 34]; thus, understanding the crosstalk between tumor cells and their m is needed to fully understand tumor development, progression, and chemoresistance in HCC. To avoid overlooking valuable drug targets due to incomplete recapitulation of the TME in experimental studies, we utilized a 3D culture system of HCC cells to identify such targets. Through proteomic analysis of HCC cells in 2D and 3D culture, we found that various types of stress in 3D HCC cultures impact energy metabolism, including expression of ASS1, which regulates arginine and citrulline metabolism [Figure 1]. Similar to our results, ASS1 was also elevated in mesothelioma 3D spheroids and in human pleural mesotheliomas, although mesothelioma is considered by many to be an ASS1-deficient tumor [35].

Because Korea ranks highest in the world in terms of liver cancer incidence and mortality rates, we also investigated the clinical value of ASS1 in Korean patients with HCC. Although most HCC samples exhibited low ASS1 expression, Korean HCC patients with increased ASS1 expression in their tumor tissue have a more favorable prognosis than those with lower expression levels [Figure 2, Supplementary Fig. 2]. ASS1 is differentially expressed across a wide range of tumors [36], the effects of which also differ in each type of tumor.

Because HCC tumors are auxotrophic for the essential amino acid arginine [37, 38], the depletion of which leads to tumor death, arginine depletion is a strategy for HCC therapy. HCCs exhibit loss of ASS1 expression via epigenetic silencing of CpG island methylation within the *ASS1* promoter [39], leading to auxotrophy [36, 40].

In this study, we sought to elucidate the novel functions of ASS1, which was upregulated in HCC spheroids. The role of ASS1 in tumor biology is unclear, as the protein may act either as a tumor suppressor [41–43] or as pro-metastatic or carcinogenic factor [44–46] in various carcinomas. Here, we demonstrated the role of ASS1 as a tumor suppressor in liver cancer. Specifically, ASS1 overexpression inhibited HCC spheroid growth and migration *in vivo* and *in vitro.* As ASS1 positivity is a biomarker of cisplatin sensitivity, ASS1 overexpression also hypersensitized HCC cells to chemotherapeutic agents [Figure 3, Table II].

Microarray analysis using HCC spheroids predicted the relationship between ER stress response and ASS1 expression in HCC spheroids. Arginine starvation induces ER stress in solid cancer cells [47], but roles of ASS1 in ER stress response have not been previously studied. As expected, ER stress in HCC spheroids not only increased ASS1 expression but also induced translocation of ASS1 from the

cytoplasm to the ER [Figure 4]. Consequently, upregulated ASS1 in HCC cells facilitated ER stress-related cell death via induction of CHOP expression independently of arginine metabolism, as well as p53 activation and NO production [Figure 6]. Although ASS1 induced susceptibility to genotoxic stress as a p53-activated gene in colorectal cancer [42] and mediated fluid shear stress by NO production [48, 49], ER stress-related cell death in ASS1-overexpressing HCC cells is independent of p53 activation and NO production. Overexpression of ASS1 exhibited stronger tumor regression in HCC with mutant p53 than in HCC with wild-type p53. Identify critical pathway to inhibit mutant p53-specific survival and growth regulatory pathways are highly promising for effective treatment of many cancers, because mutant p53 often exhibits novel gain-of-functions to promote tumor growth and metastasis. Hence, the increased tumor suppression by ASS1 overexpression in HCC with mutant p53 was unusual and very valuable new pathway to overcome mutant p53-specific survival pathways.

The ER stress-mediated upregulation of ASS1 in HCC spheroids restricted their growth through ER stress-induced apoptosis via increased expression of CHOP. Thus, we thought that targeting the upregulation of ASS1 may represent a promising strategy for HCC therapy. Indeed, treatment with the hypomethylating agent decitabine both enhanced ASS1 expression and improved the efficacy of cisplatin against HCC cells [Figure 7, 8].

Conclusions

Our results provide clear evidence that the low ASS1 expression level in HCC tissue negatively impacted the overall survival of patients with liver cancer. Moreover, we discovered novel functions of ASS1 as a tumor suppressor through its arginine-metabolism–independent facilitation of ER stress-induced apoptosis in mutant p53 HCCs [Figure 9]. Therefore, we conclude that identifying compounds that increase ASS1 expression may be a promising approach for enhancing HCC therapy.

Abbreviations

ALDOA
aldolase A
ASNS
asparagine synthetase
ASS1
argininosuccinate synthase 1
ATF3
activating transcription factor 3
ATF4
activating transcription factor 4
ATF6
activating transcription factor 6
CALR

calreticulin
CHOP
C/EBP Homologous Protein
cPTIO
carboxy-PTIO
CTLA-4
cytotoxic T-lymphocyte-associated protein 4
eIF2α
eukaryotic initiation factor 2α
ECM
extracellular matrix
EMT
epithelial-to-mesenchymal transition
ER
endoplasmic reticulum
FDA
food and drug administration
GRP78
Glucose-Regulated Protein 78
HCC
Hepatocellular carcinoma
HSF5
heat shock transcription factor 5
HSP90B1
heat shock protein 90 beta family member 1
HSPA1A
heat shock protein family A member 1A
HSPA5
heat shock protein family A member 5
HSPD1
heat shock protein family D member 1
IF
Immunofluorescence
IND
investigational new drug application; α-SMA
IRE1
inositol-requiring enzyme-1
LOPAC
Library of Pharmacologically Active Compounds
mTOR

mammalian target of rapamycin
NO
nitric oxide
PARP
poly ADP-ribose polymerase
PD-1
programmed cell death protein 1
PD-L1
programmed death-ligand 1
PERK
PKR-like ER kinase
PI3K
Phosphoinositide 3-kinases
PTEN
Phosphatase and tensin homolog
S1P
site-1 protease
S2P
site-2 protease
TCGA
The Cancer Genome Atlas
TG
thapsigargin
TGF
transforming growth factor
TM
tunicamycin
TME
tumor microenvironment
UPR
unfolded protein response
VEGF
vascular endothelial growth factor
VEGFR
vascular endothelial growth factor receptor
XBP1
x-box binding protein 1

Declarations

Consent for publication

All authors read and approved the final manuscript for publication.

Availability of data and materials

Information is included in the Methods section.

Competing interests

The authors declare that they have no competing interests.

Funding

This work was supported by the National Research foundation of Korea (NRF) grant funded by the Korea government (MSIP) (2017M3A9G7072864 and NRF-2017M3A9G6068246) and Gyeonggi-do

Authors' contributions

SK, ML, YS and SY-L designed the *in vitro* experiments, analyzed data and prepared the manuscript. SK performed cell culture and participated in the *in vivo* experiments. IC performed microarray and bioinformatics analysis. IP and JK performed high throughput screening. JK and KK provided the HCC patient tissues and participated in HCC primary cells analysis and characterization. KK and HS designed and was the overseer of the entire study.

Ethics approval and patient consent

This study was conducted in accordance with the Declaration of Helsinki, and samples were provided from patients of ASAN medical center. Approximately 60 patients with a diagnosis of liver cancer who were treated and followed up in the clinic participated. The study was approved by the Human Research Ethic Committee of ASAN medical center (Permit Number: 2007-0332). The Institutional Review Board of ASAN medical center complies with the related laws including ICH, KGCP, and the Bioethics and Safety Act of Korea. Written informed consent for the use of tissues for research purposes was obtained from patients at the time of tumor specimen procurement.

Acknowledgements "Not applicable"

References

1. Cheng AL, Kang YK, Chen Z, Tsao CJ, Qin S, Kim JS, Luo R, Feng J, Ye S, Yang TS *et al*: **Efficacy and safety of sorafenib in patients in the Asia-Pacific region with advanced hepatocellular carcinoma: a phase III randomised, double-blind, placebo-controlled trial**. *The Lancet Oncology* 2009, **10**(1):25-34.
2. Tsun ZY, Possemato R: **Amino acid management in cancer**. *Seminars in cell & developmental biology* 2015, **43**:22-32.

3. Amelio I, Cutruzzola F, Antonov A, Agostini M, Melino G: **Serine and glycine metabolism in cancer**. *Trends in biochemical sciences* 2014, **39**(4):191-198.
4. Wise DR, Thompson CB: **Glutamine addiction: a new therapeutic target in cancer**. *Trends in biochemical sciences* 2010, **35**(8):427-433.
5. Lind DS: **Arginine and cancer**. *The Journal of nutrition* 2004, **134**(10 Suppl):2837S-2841S; discussion 2853S.
6. Jobgen WS, Fried SK, Fu WJ, Meininger CJ, Wu G: **Regulatory role for the arginine-nitric oxide pathway in metabolism of energy substrates**. *The Journal of nutritional biochemistry* 2006, **17**(9):571-588.
7. Leuzzi V, Alessandri MG, Casarano M, Battini R, Cioni G: **Arginine and glycine stimulate creatine synthesis in creatine transporter 1-deficient lymphoblasts**. *Analytical biochemistry* 2008, **375**(1):153-155.
8. Rozpedek W, Pytel D, Mucha B, Leszczynska H, Diehl JA, Majsterek I: **The Role of the PERK/eIF2alpha/ATF4/CHOP Signaling Pathway in Tumor Progression During Endoplasmic Reticulum Stress**. *Curr Mol Med* 2016, **16**(6):533-544.
9. Sicari D, Fantuz M, Bellazzo A, Valentino E, Apollonio M, Pontisso I, Di Cristino F, Dal Ferro M, Bicciato S, Del Sal G *et al*: **Mutant p53 improves cancer cells' resistance to endoplasmic reticulum stress by sustaining activation of the UPR regulator ATF6**. *Oncogene* 2019, **38**(34):6184-6195.
10. Cubillos-Ruiz JR, Bettigole SE, Glimcher LH: **Molecular Pathways: Immunosuppressive Roles of IRE1alpha-XBP1 Signaling in Dendritic Cells of the Tumor Microenvironment**. *Clin Cancer Res* 2016, **22**(9):2121-2126.
11. Hetz C: **The unfolded protein response: controlling cell fate decisions under ER stress and beyond**. *Nature reviews Molecular cell biology* 2012, **13**(2):89-102.
12. Pino SC, O'Sullivan-Murphy B, Lidstone EA, Yang C, Lipson KL, Jurczyk A, diIorio P, Brehm MA, Mordes JP, Greiner DL *et al*: **CHOP mediates endoplasmic reticulum stress-induced apoptosis in Gimap5-deficient T cells**. *PloS one* 2009, **4**(5):e5468.
13. Marciniak SJ, Yun CY, Oyadomari S, Novoa I, Zhang Y, Jungreis R, Nagata K, Harding HP, Ron D: **CHOP induces death by promoting protein synthesis and oxidation in the stressed endoplasmic reticulum**. *Genes & development* 2004, **18**(24):3066-3077.
14. Liu L, Qin S, Zheng Y, Han L, Zhang M, Luo N, Liu Z, Gu N, Gu X, Yin X: **Molecular targeting of VEGF/VEGFR signaling by the anti-VEGF monoclonal antibody BD0801 inhibits the growth and induces apoptosis of human hepatocellular carcinoma cells in vitro and in vivo**. *Cancer biology & therapy* 2017, **18**(3):166-176.
15. Cao G, Li X, Qin C, Li J: **Prognostic Value of VEGF in Hepatocellular Carcinoma Patients Treated with Sorafenib: A Meta-Analysis**. *Medical science monitor : international medical journal of experimental and clinical research* 2015, **21**:3144-3151.
16. Finn RS, Zhu AX: **Targeting angiogenesis in hepatocellular carcinoma: focus on VEGF and bevacizumab**. *Expert review of anticancer therapy* 2009, **9**(4):503-509.

17. Zhu AX, Duda DG, Sahani DV, Jain RK: **HCC and angiogenesis: possible targets and future directions**. *Nature reviews Clinical oncology* 2011, **8**(5):292-301.
18. Wilhelm SM, Adnane L, Newell P, Villanueva A, Llovet JM, Lynch M: **Preclinical overview of sorafenib, a multikinase inhibitor that targets both Raf and VEGF and PDGF receptor tyrosine kinase signaling**. *Molecular cancer therapeutics* 2008, **7**(10):3129-3140.
19. Wilhelm S, Carter C, Lynch M, Lowinger T, Dumas J, Smith RA, Schwartz B, Simantov R, Kelley S: **Discovery and development of sorafenib: a multikinase inhibitor for treating cancer**. *Nature reviews Drug discovery* 2006, **5**(10):835-844.
20. Zhu YJ, Zheng B, Wang HY, Chen L: **New knowledge of the mechanisms of sorafenib resistance in liver cancer**. *Acta pharmacologica Sinica* 2017, **38**(5):614-622.
21. Kudo M, Finn RS, Qin S, Han KH, Ikeda K, Piscaglia F, Baron A, Park JW, Han G, Jassem J *et al*: **Lenvatinib versus sorafenib in first-line treatment of patients with unresectable hepatocellular carcinoma: a randomised phase 3 non-inferiority trial**. *Lancet* 2018, **391**(10126):1163-1173.
22. Bruix J, Qin S, Merle P, Granito A, Huang YH, Bodoky G, Pracht M, Yokosuka O, Rosmorduc O, Breder V *et al*: **Regorafenib for patients with hepatocellular carcinoma who progressed on sorafenib treatment (RESORCE): a randomised, double-blind, placebo-controlled, phase 3 trial**. *Lancet* 2017, **389**(10064):56-66.
23. Zhu AX, Park JO, Ryoo BY, Yen CJ, Poon R, Pastorelli D, Blanc JF, Chung HC, Baron AD, Pfiffer TE *et al*: **Ramucirumab versus placebo as second-line treatment in patients with advanced hepatocellular carcinoma following first-line therapy with sorafenib (REACH): a randomised, double-blind, multicentre, phase 3 trial**. *The Lancet Oncology* 2015, **16**(7):859-870.
24. Abou-Alfa GK, Meyer T, Cheng AL, El-Khoueiry AB, Rimassa L, Ryoo BY, Cicin I, Merle P, Chen Y, Park JW *et al*: **Cabozantinib in Patients with Advanced and Progressing Hepatocellular Carcinoma**. *The New England journal of medicine* 2018, **379**(1):54-63.
25. Okazaki T, Honjo T: **PD-1 and PD-1 ligands: from discovery to clinical application**. *International immunology* 2007, **19**(7):813-824.
26. El-Khoueiry AB, Sangro B, Yau T, Crocenzi TS, Kudo M, Hsu C, Kim TY, Choo SP, Trojan J, Welling THR *et al*: **Nivolumab in patients with advanced hepatocellular carcinoma (CheckMate 040): an open-label, non-comparative, phase 1/2 dose escalation and expansion trial**. *Lancet* 2017, **389**(10088):2492-2502.
27. Takahashi T, Tagami T, Yamazaki S, Uede T, Shimizu J, Sakaguchi N, Mak TW, Sakaguchi S: **Immunologic self-tolerance maintained by CD25(+)CD4(+) regulatory T cells constitutively expressing cytotoxic T lymphocyte-associated antigen 4**. *The Journal of experimental medicine* 2000, **192**(2):303-310.
28. Xu F, Jin T, Zhu Y, Dai C: **Immune checkpoint therapy in liver cancer**. *Journal of experimental & clinical cancer research : CR* 2018, **37**(1):110.
29. Bouattour M, Raymond E, Qin S, Cheng AL, Stammberger U, Locatelli G, Faivre S: **Recent developments of c-Met as a therapeutic target in hepatocellular carcinoma**. *Hepatology* 2018,

67(3):1132-1149.

30. Giannelli G, Villa E, Lahn M: **Transforming growth factor-beta as a therapeutic target in hepatocellular carcinoma**. *Cancer research* 2014, **74**(7):1890-1894.
31. Chen JS, Wang Q, Fu XH, Huang XH, Chen XL, Cao LQ, Chen LZ, Tan HX, Li W, Bi J *et al*: **Involvement of PI3K/PTEN/AKT/mTOR pathway in invasion and metastasis in hepatocellular carcinoma: Association with MMP-9**. *Hepatology research : the official journal of the Japan Society of Hepatology* 2009, **39**(2):177-186.
32. Della Corte CM, Viscardi G, Papaccio F, Esposito G, Martini G, Ciardiello D, Martinelli E, Ciardiello F, Morgillo F: **Implication of the Hedgehog pathway in hepatocellular carcinoma**. *World journal of gastroenterology* 2017, **23**(24):4330-4340.
33. Gouirand V, Guillaumond F, Vasseur S: **Influence of the Tumor Microenvironment on Cancer Cells Metabolic Reprogramming**. *Frontiers in oncology* 2018, **8**:117.
34. Yang LV: **Tumor Microenvironment and Metabolism**. *International journal of molecular sciences* 2017, **18**(12).
35. Barbone D, Van Dam L, Follo C, Jithesh PV, Zhang SD, Richards WG, Bueno R, Fennell DA, Broaddus VC: **Analysis of Gene Expression in 3D Spheroids Highlights a Survival Role for ASS1 in Mesothelioma**. *PloS one* 2016, **11**(3):e0150044.
36. Delage B, Fennell DA, Nicholson L, McNeish I, Lemoine NR, Crook T, Szlosarek PW: **Arginine deprivation and argininosuccinate synthetase expression in the treatment of cancer**. *International journal of cancer* 2010, **126**(12):2762-2772.
37. Barbul A: **Arginine: biochemistry, physiology, and therapeutic implications**. *JPEN Journal of parenteral and enteral nutrition* 1986, **10**(2):227-238.
38. Cheng PN, Leung YC, Lo WH, Tsui SM, Lam KC: **Remission of hepatocellular carcinoma with arginine depletion induced by systemic release of endogenous hepatic arginase due to transhepatic arterial embolisation, augmented by high-dose insulin: arginase as a potential drug candidate for hepatocellular carcinoma**. *Cancer letters* 2005, **224**(1):67-80.
39. Delage B, Luong P, Maharaj L, O'Riain C, Syed N, Crook T, Hatzimichael E, Papoudou-Bai A, Mitchell TJ, Whittaker SJ *et al*: **Promoter methylation of argininosuccinate synthetase-1 sensitises lymphomas to arginine deiminase treatment, autophagy and caspase-dependent apoptosis**. *Cell death & disease* 2012, **3**:e342.
40. Dillon BJ, Prieto VG, Curley SA, Ensor CM, Holtsberg FW, Bomalaski JS, Clark MA: **Incidence and distribution of argininosuccinate synthetase deficiency in human cancers: a method for identifying cancers sensitive to arginine deprivation**. *Cancer* 2004, **100**(4):826-833.
41. Huang HY, Wu WR, Wang YH, Wang JW, Fang FM, Tsai JW, Li SH, Hung HC, Yu SC, Lan J *et al*: **ASS1 as a novel tumor suppressor gene in myxofibrosarcomas: aberrant loss via epigenetic DNA methylation confers aggressive phenotypes, negative prognostic impact, and therapeutic relevance**. *Clinical cancer research : an official journal of the American Association for Cancer Research* 2013, **19**(11):2861-2872.

42. Miyamoto T, Lo PHY, Saichi N, Ueda K, Hirata M, Tanikawa C, Matsuda K: **Argininosuccinate synthase 1 is an intrinsic Akt repressor transactivated by p53**. *Science advances* 2017, **3**(5):e1603204.
43. Kobayashi E, Masuda M, Nakayama R, Ichikawa H, Satow R, Shitashige M, Honda K, Yamaguchi U, Shoji A, Tochigi N *et al*: **Reduced argininosuccinate synthetase is a predictive biomarker for the development of pulmonary metastasis in patients with osteosarcoma**. *Molecular cancer therapeutics* 2010, **9**(3):535-544.
44. Shan YS, Hsu HP, Lai MD, Yen MC, Chen WC, Fang JH, Weng TY, Chen YL: **Argininosuccinate synthetase 1 suppression and arginine restriction inhibit cell migration in gastric cancer cell lines**. *Scientific reports* 2015, **5**:9783.
45. Tsai CY, Chi HC, Chi LM, Yang HY, Tsai MM, Lee KF, Huang HW, Chou LF, Cheng AJ, Yang CW *et al*: **Argininosuccinate synthetase 1 contributes to gastric cancer invasion and progression by modulating autophagy**. *FASEB journal : official publication of the Federation of American Societies for Experimental Biology* 2018, **32**(5):2601-2614.
46. Szlosarek PW, Grimshaw MJ, Wilbanks GD, Hagemann T, Wilson JL, Burke F, Stamp G, Balkwill FR: **Aberrant regulation of argininosuccinate synthetase by TNF-alpha in human epithelial ovarian cancer**. *International journal of cancer* 2007, **121**(1):6-11.
47. Bobak Y, Kurlishchuk Y, Vynnytska-Myronovska B, Grydzuk O, Shuvayeva G, Redowicz MJ, Kunz-Schughart LA, Stasyk O: **Arginine deprivation induces endoplasmic reticulum stress in human solid cancer cells**. *The international journal of biochemistry & cell biology* 2016, **70**:29-38.
48. Mun GI, Kim IS, Lee BH, Boo YC: **Endothelial argininosuccinate synthetase 1 regulates nitric oxide production and monocyte adhesion under static and laminar shear stress conditions**. *The Journal of biological chemistry* 2011, **286**(4):2536-2542.
49. Mun GI, Boo YC: **A regulatory role of Kruppel-like factor 4 in endothelial argininosuccinate synthetase 1 expression in response to laminar shear stress**. *Biochemical and biophysical research communications* 2012, **420**(2):450-455.

Figures

Figure 1.

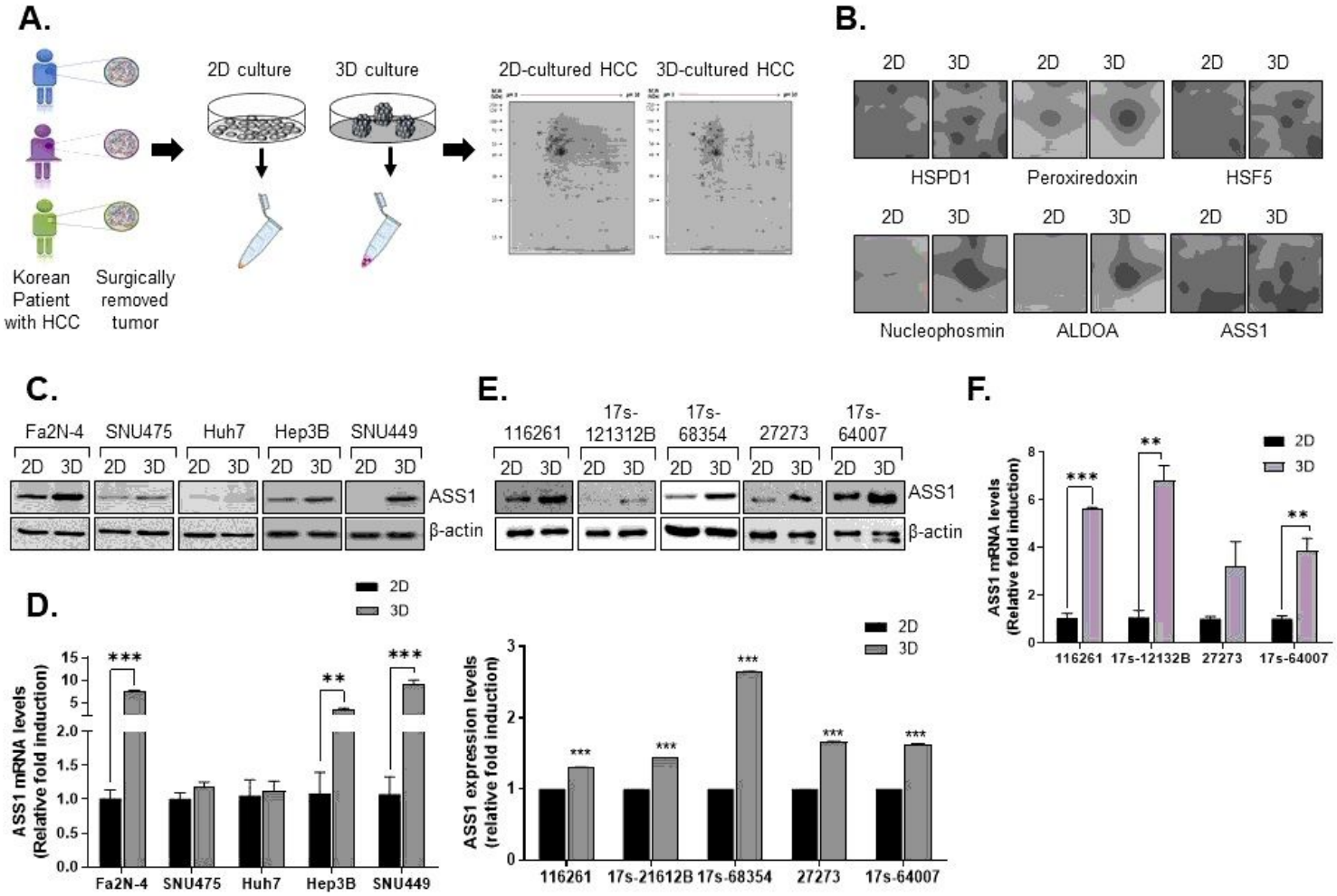

Figure 1

Expression of ASS1 is upregulated in HCC spheroids (A) Schematic of the proteomics analysis of Korean patient-derived HCC cells cultured in monolayers (2D) or spheroids (3D). (B) Expression of identified proteins including HSPD1, peroxiredoxin, HSF5, Nucleophosmin, ALDOA, and ASS1 in 2D or 3D-cultured HCC. Expression of ASS1 in 2D or 3D-culured system from Fa2N-4 and HCC cell lines (C) by western blot assay and (D) by qRT-PCR. Expression of ASS1 in patient-derived HCC cell lines (E) by western blot and (F) qRT-PCR. **P<0.01 and ***P<0.001 compared to control groups.

Figure 1.

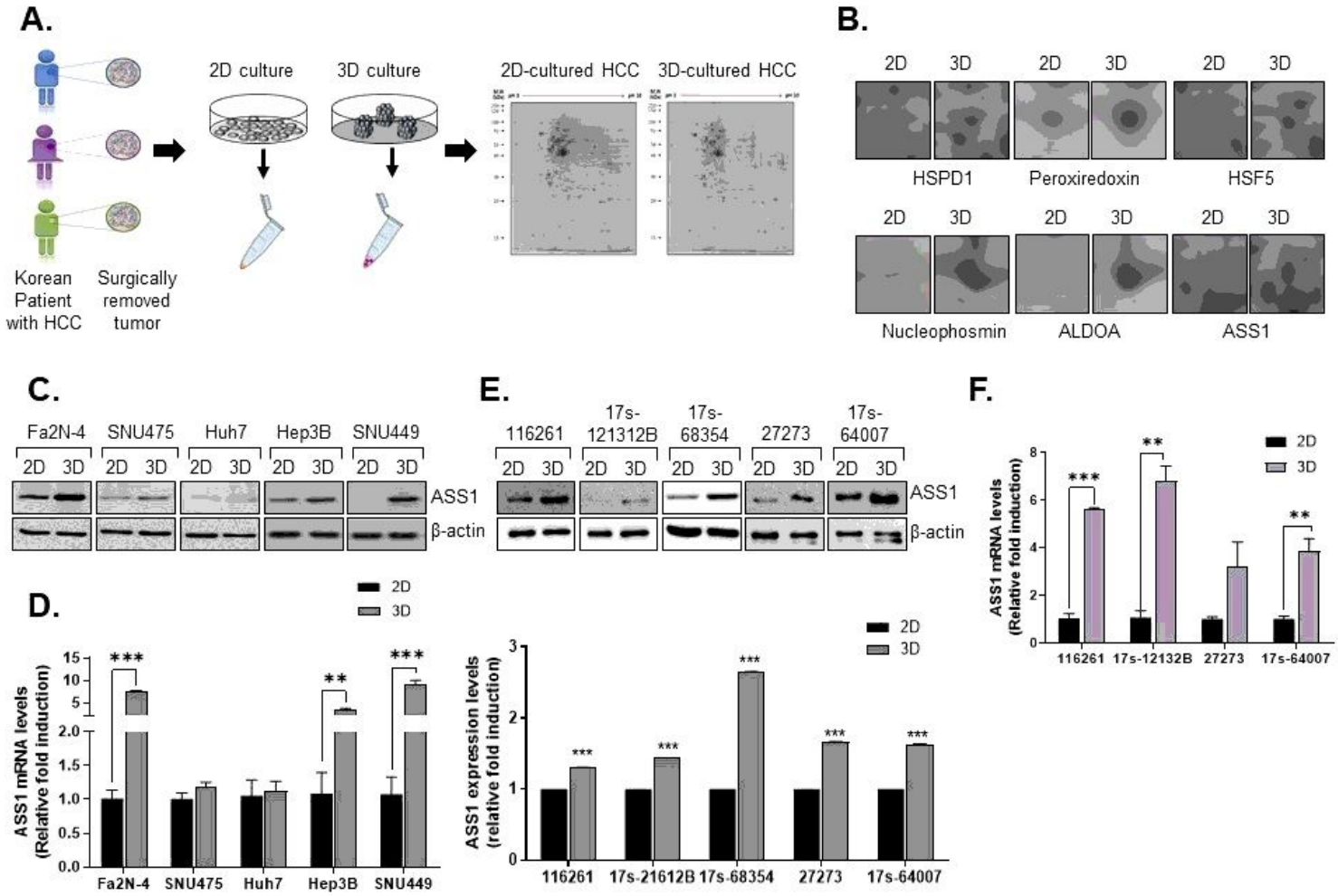

Figure 1

Expression of ASS1 is upregulated in HCC spheroids (A) Schematic of the proteomics analysis of Korean patient-derived HCC cells cultured in monolayers (2D) or spheroids (3D). (B) Expression of identified proteins including HSPD1, peroxiredoxin, HSF5, Nucleophosmin, ALDOA, and ASS1 in 2D or 3D-cultured HCC. Expression of ASS1 in 2D or 3D-culured system from Fa2N-4 and HCC cell lines (C) by western blot assay and (D) by qRT-PCR. Expression of ASS1 in patient-derived HCC cell lines (E) by western blot and (F) qRT-PCR. **P<0.01 and ***P<0.001 compared to control groups.

Figure 2.

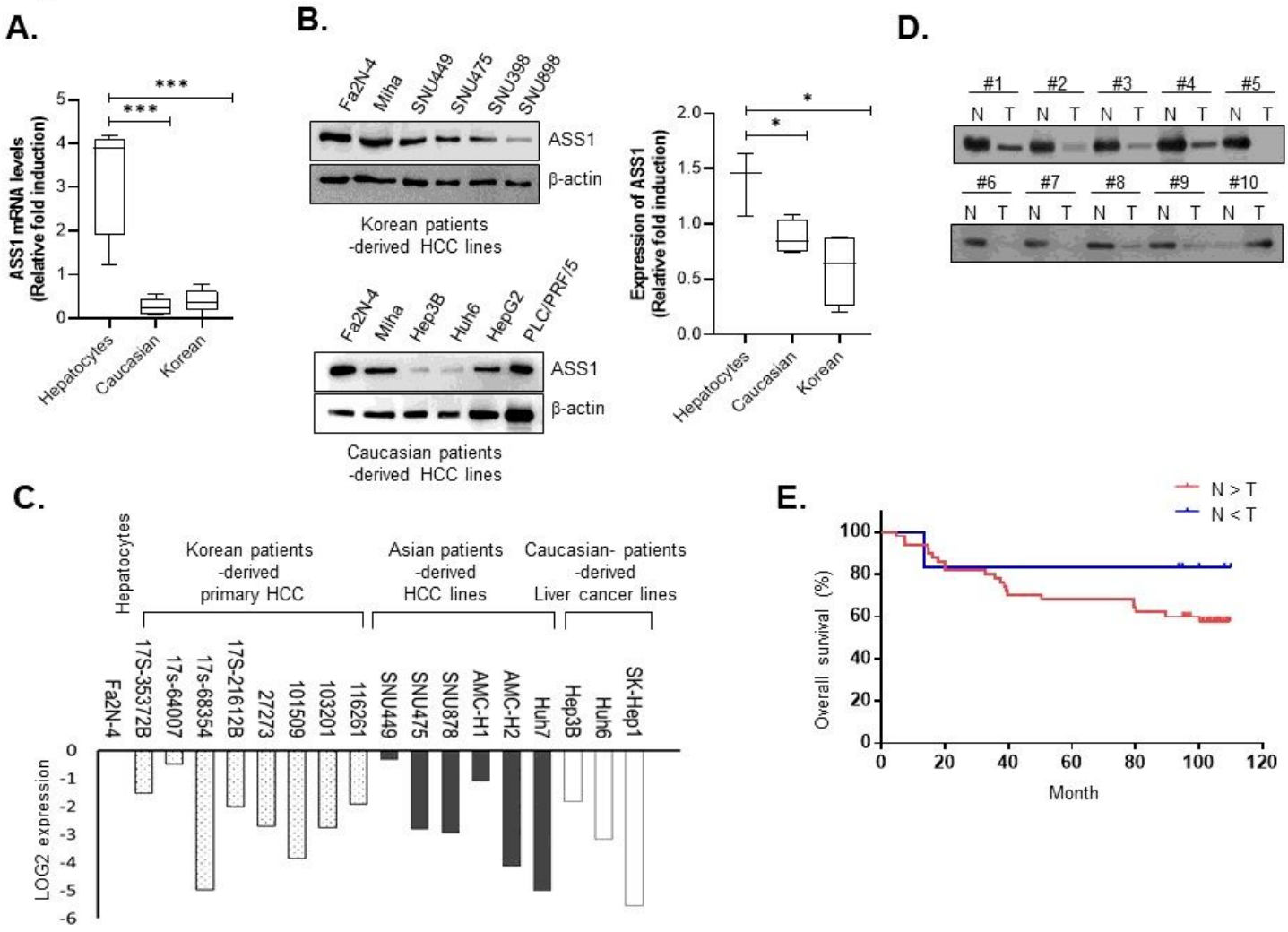

Figure 2

Patients with increased ASS1 expression in HCC have a more favorable prognosis (A) ASS1 mRNA expression levels and (B) expression of ASS1 in hepatocytes; Fa2N-4, miha., Caucasian-derived HCC cells ;Hep3B, Huh6, HepG2, and PLC/PRF/5, and Korean-derived HCC cells;SNU449, SNU475, SNU398, and SNU898. (C) ASS1 mRNA expression levels in tumor spheroids from eight Korean patient-derived HCC cell lines, six Asian patient-derived HCC cell lines (SNU449, SNU475, SNU878, Huh7, AMC-H1, AMC-H2), three Caucasian patient-derived HCC cell lines (Hep3B, Huh6, SKhep-1), and normal hepatocytes (Fa2N-4). (D) Protein expression of ASS1 in adjacent non-tumor tissues (N) and tumor tissues (T) from HCC patient samples by western blot analysis. (E) 10-year overall survival rates of patients with high vs. low expression of ASS1. (N=peritumoral tissues, T=tumor tissues) *P<0.05 and ***P<0.001 compared to control group.

Figure 2.

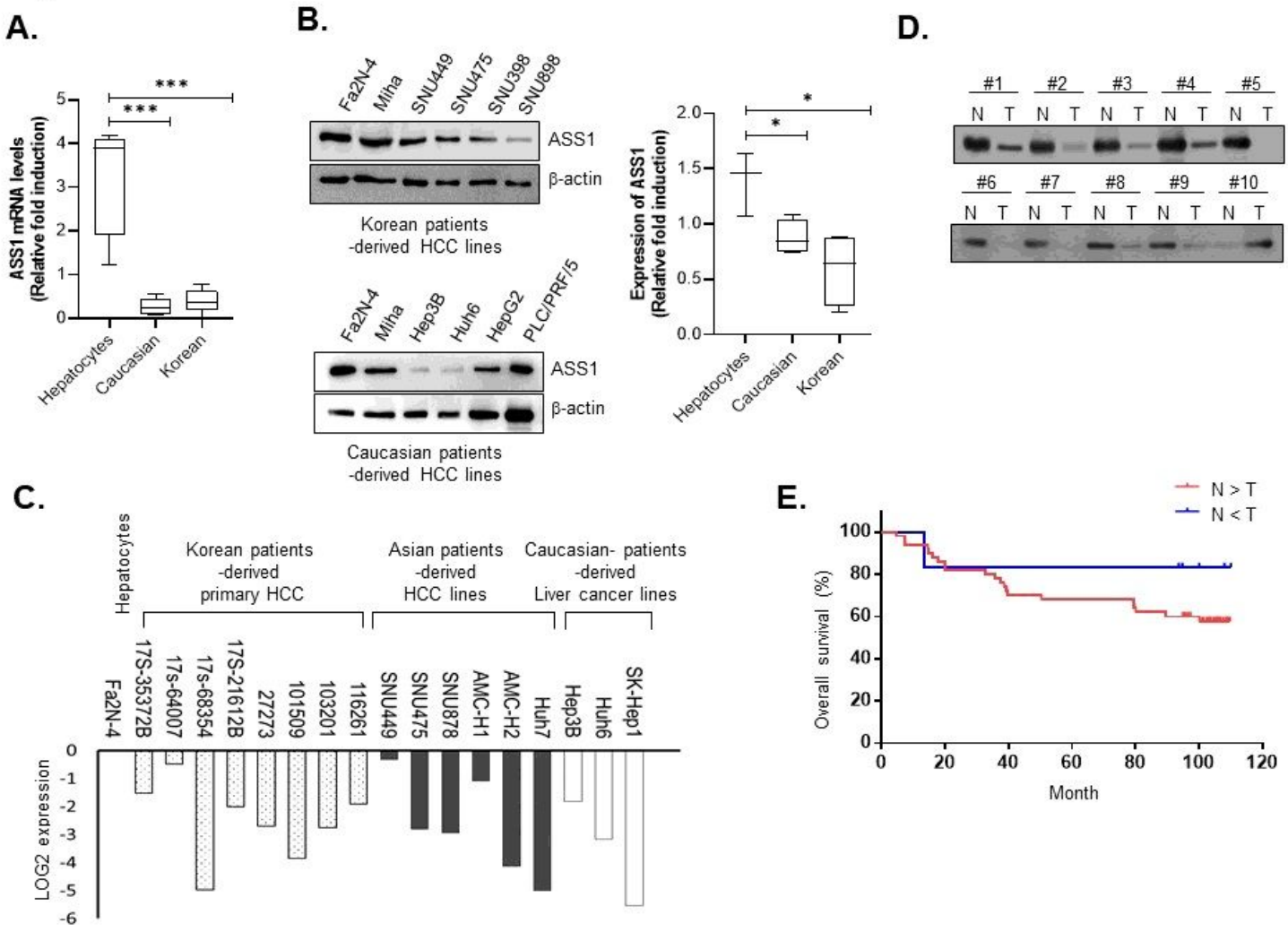

Figure 2

Patients with increased ASS1 expression in HCC have a more favorable prognosis (A) ASS1 mRNA expression levels and (B) expression of ASS1 in hepatocytes; Fa2N-4, miha., Caucasian-derived HCC cells ;Hep3B, Huh6, HepG2, and PLC/PRF/5, and Korean-derived HCC cells;SNU449, SNU475, SNU398, and SNU898. (C) ASS1 mRNA expression levels in tumor spheroids from eight Korean patient-derived HCC cell lines, six Asian patient-derived HCC cell lines (SNU449, SNU475, SNU878, Huh7, AMC-H1, AMC-H2), three Caucasian patient-derived HCC cell lines (Hep3B, Huh6, SKhep-1), and normal hepatocytes (Fa2N-4). (D) Protein expression of ASS1 in adjacent non-tumor tissues (N) and tumor tissues (T) from HCC patient samples by western blot analysis. (E) 10-year overall survival rates of patients with high vs. low expression of ASS1. (N=peritumoral tissues, T=tumor tissues) *P<0.05 and ***P<0.001 compared to control group.

Figure 3.

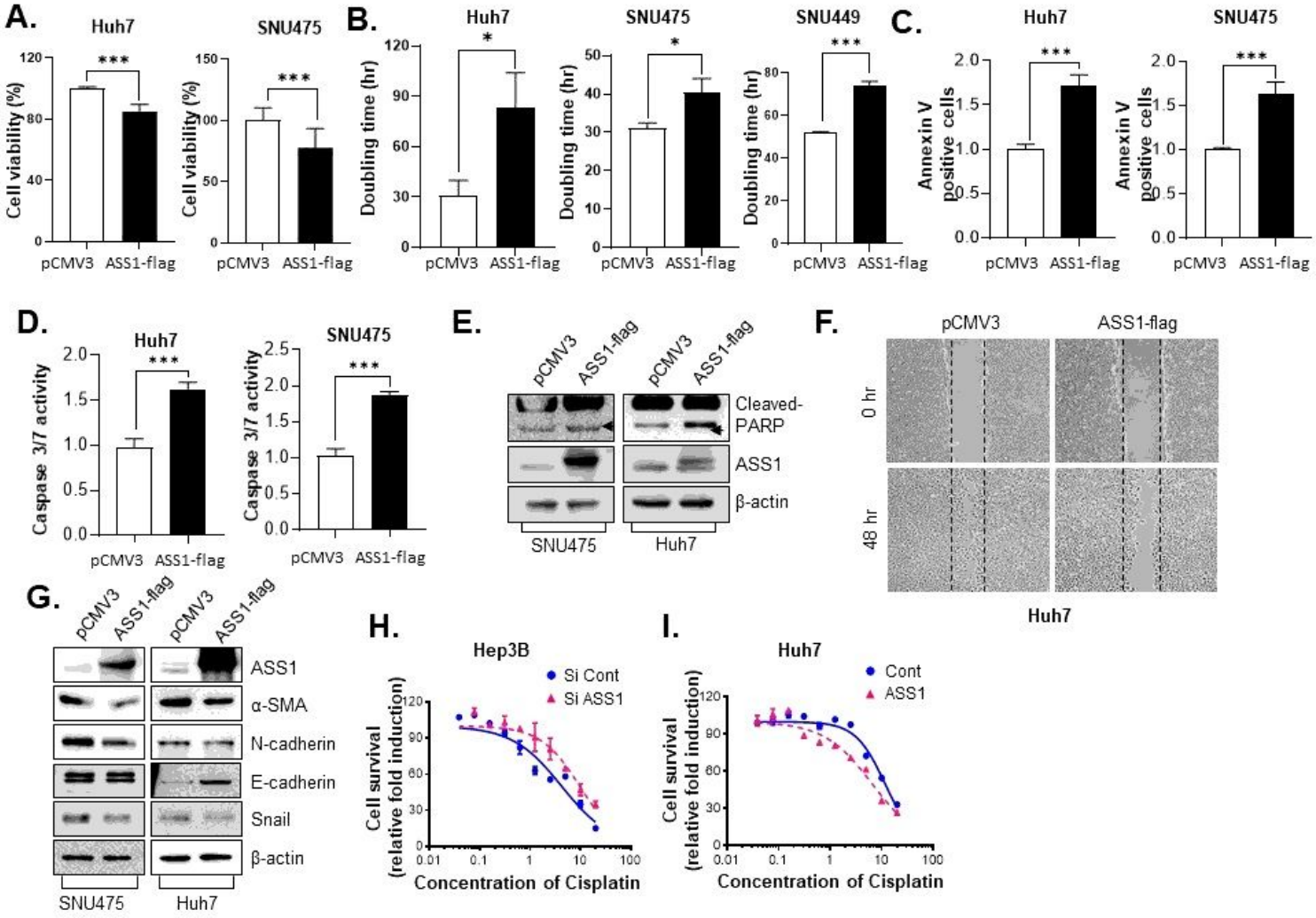

Figure 3

Overexpression of ASS1 inhibits HCC tumor growth and improves chemotherapy efficiency (A) Cell viability analysis of Huh7 and SNU475 and (B) doubling time analysis of Huh7 cells, SNU475 cells and SNU449 cells transfected with pCMV3 or ASS1-flag. The measurement of (C) Annexin V staining apoptosis analysis, (D) Caspase3/7 activity and (E) Expression of cleaved PARP of Huh7 cells and SNU475 cells transfected with pCMV3 or ASS1-flag. (F) Wound healing assays of Huh7 cells transfected with pCMV3 or ASS1-Flag. (G) Expression of EMT-related proteins, including a-SMA, N-cadherin, E-cadherin, and Snail-1 in Huh7 and SNU475 cells transfected with pCMV3 or ASS1-Flag. Cell survival curves of (H) siRNA against ASS1-transfected in Hep3B cells and (I) ASS1 transfected in Huh7 cells treated with cisplatin at the indicated concentrations. *P<0.05, **P<0.01 and ***P<0.001 compared to control group.

Figure 3.

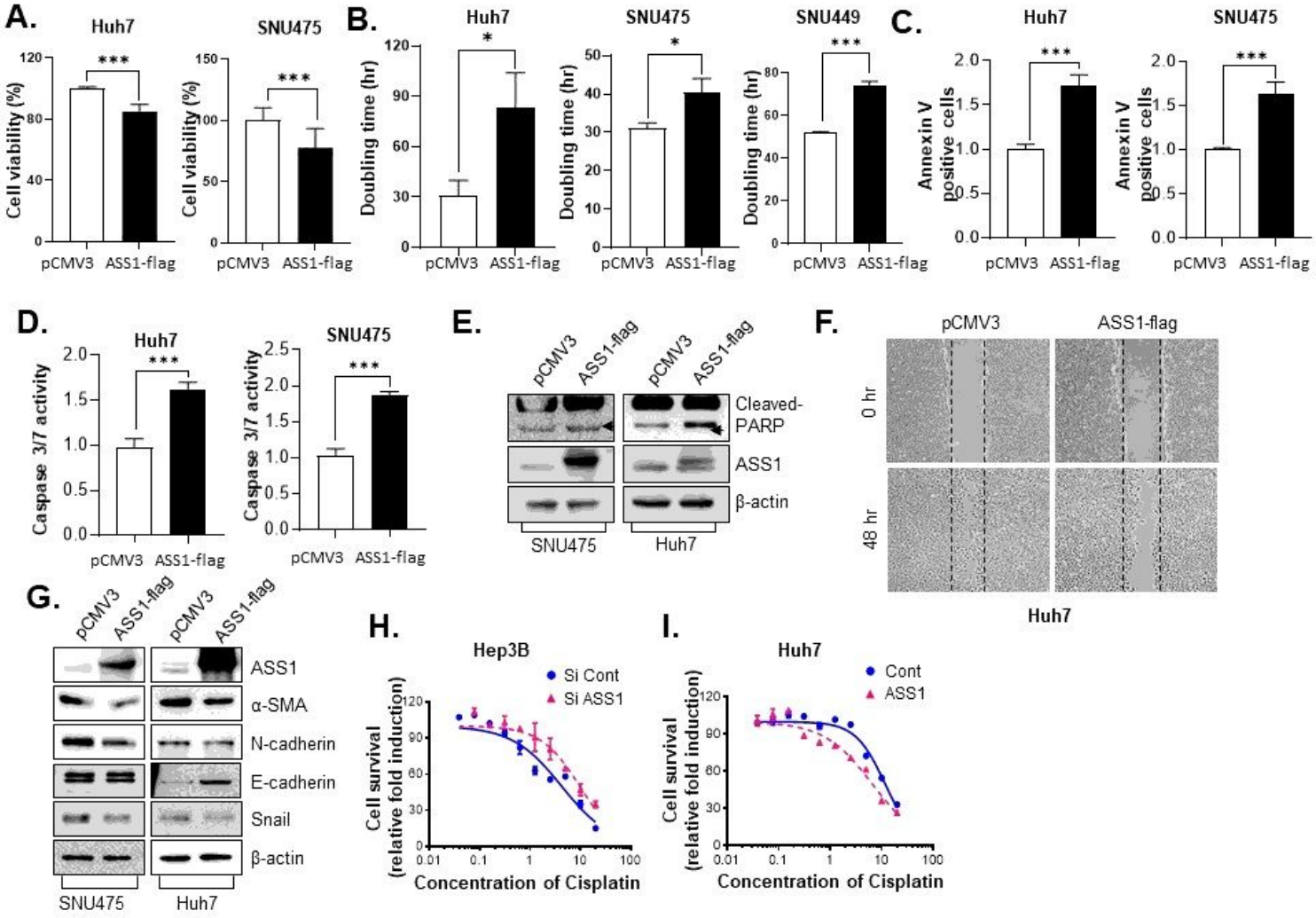

Figure 3

Overexpression of ASS1 inhibits HCC tumor growth and improves chemotherapy efficiency (A) Cell viability analysis of Huh7 and SNU475 and (B) doubling time analysis of Huh7 cells, SNU475 cells and SNU449 cells transfected with pCMV3 or ASS1-flag. The measurement of (C) Annexin V staining apoptosis analysis, (D) Caspase3/7 activity and (E) Expression of cleaved PARP of Huh7 cells and SNU475 cells transfected with pCMV3 or ASS1-flag. (F) Wound healing assays of Huh7 cells transfected with pCMV3 or ASS1-Flag. (G) Expression of EMT-related proteins, including a-SMA, N-cadherin, E-cadherin, and Snail-1 in Huh7 and SNU475 cells transfected with pCMV3 or ASS1-Flag. Cell survival curves of (H) siRNA against ASS1-transfected in Hep3B cells and (I) ASS1 transfected in Huh7 cells treated with cisplatin at the indicated concentrations. *P<0.05, **P<0.01 and ***P<0.001 compared to control group.

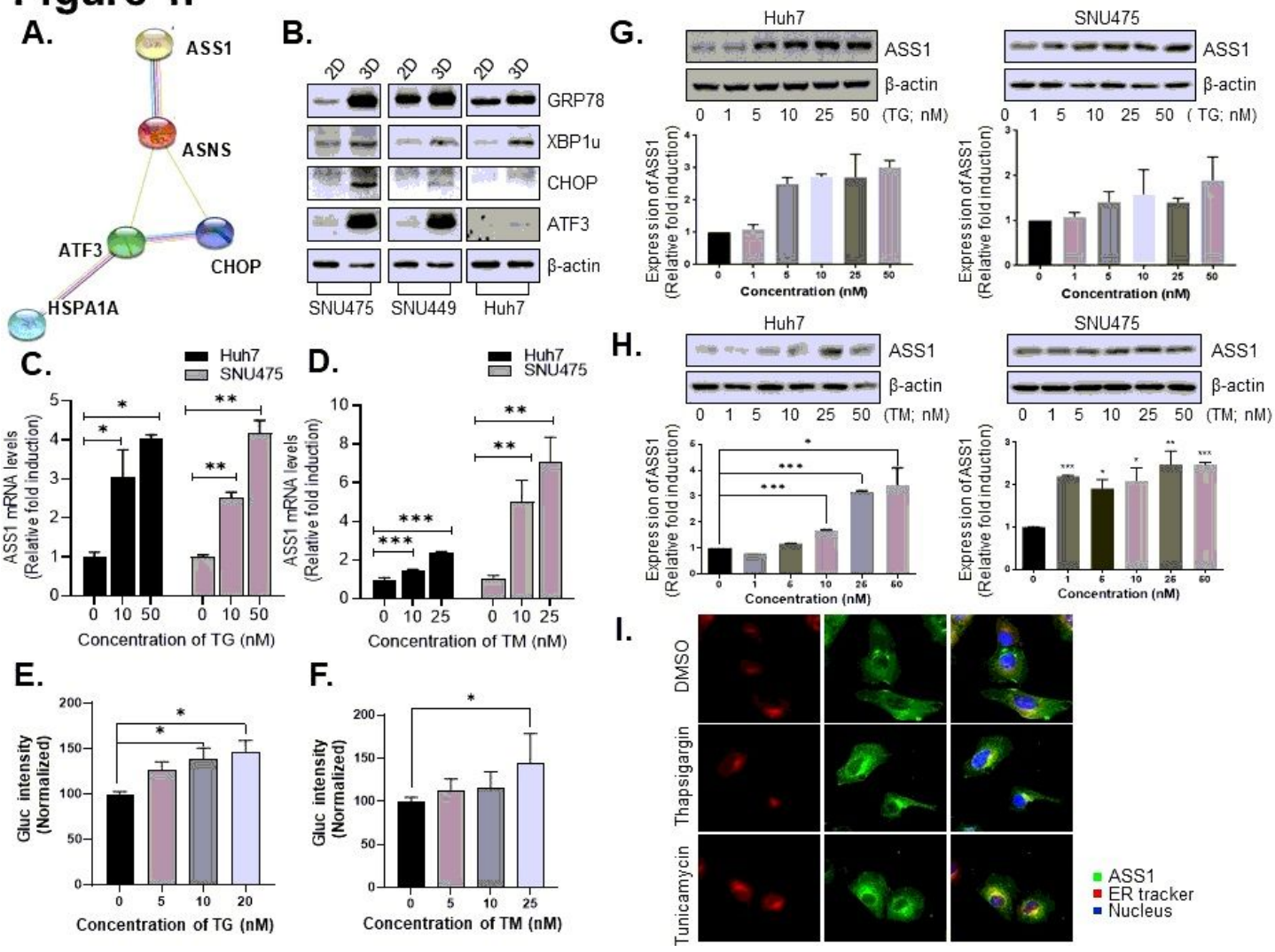

Figure 4

ASS1 is upregulated through ER stress response in HCC spheroids (A) Microarray analysis of ASS1-overexpressing HCC spheroids implicated four genes for further study (ASNS, ATF3, CHOP, and HSPA1A). (B) Expression of ER stress response related proteins; GRP78, XBP1s, CHOP and ATF3 in monolayers (2D) or spheroids (3D) of HCC cell lines including SNU475 cells, SNU449 cells and Huh7 cells. (C-D) ASS1 mRNA levels by RT-PCR analysis in Huh7 cells and SNU475 cells with treatment of ER stress inducers; TG and TM. (E-F) ASS1 promoter activity by luciferase assay in Huh7 cells with treatment of TG and TM. ASS1 expression levels in Huh7 cells and SNU475 cells with treatment of (G) TG and (H) TM. (I) Immunofluorescence (IF) images showing ASS1 (green), ER (red), and nuclei (blue) in Huh7 cells after ER stress induction by TG and TM treatment. *P<0.05, **P<0.01 and ***P<0.001 compared to control group. TG;thapsigargin, TM;tunicamycin.

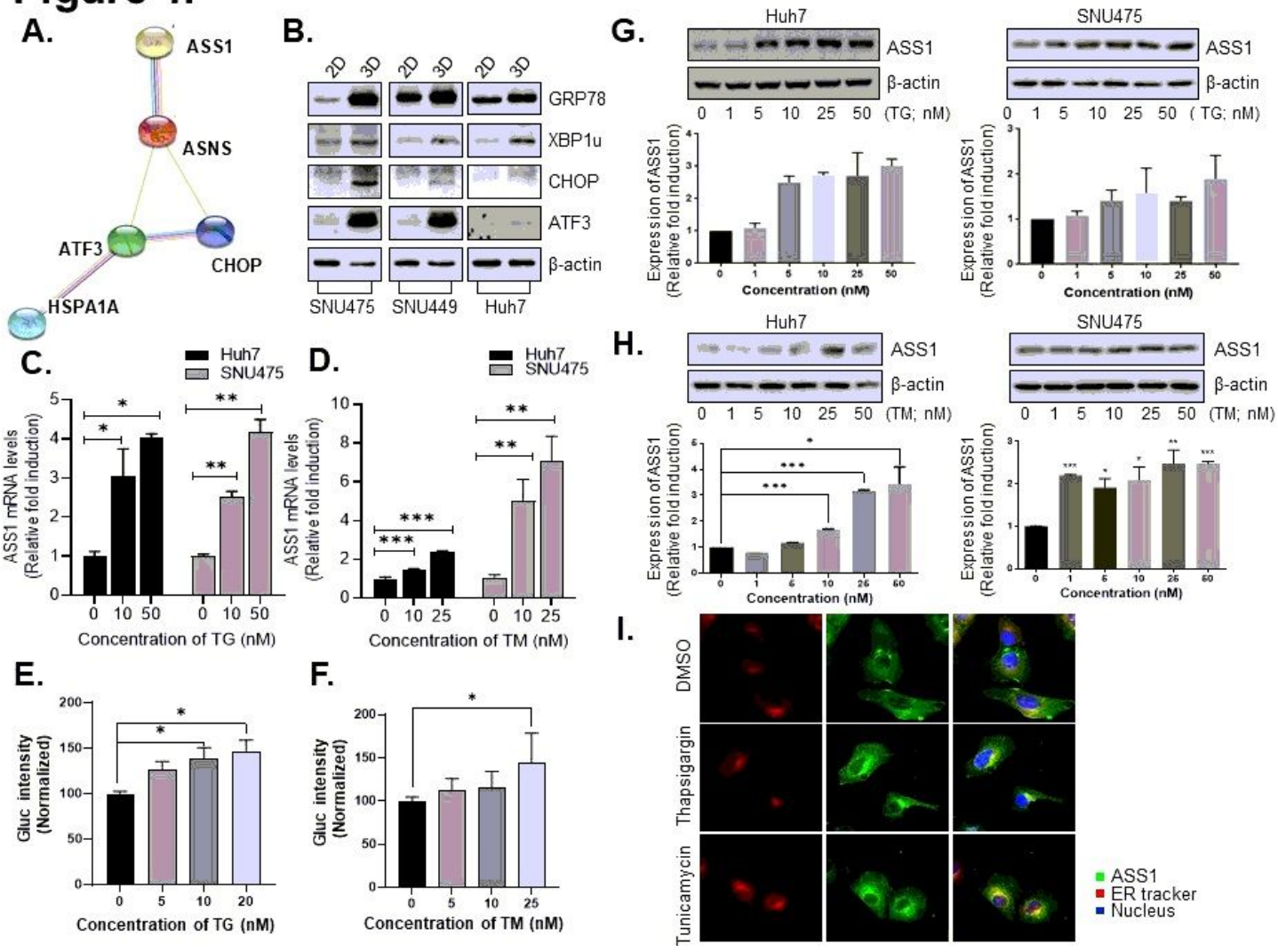

Figure 4

ASS1 is upregulated through ER stress response in HCC spheroids (A) Microarray analysis of ASS1-overexpressing HCC spheroids implicated four genes for further study (ASNS, ATF3, CHOP, and HSPA1A). (B) Expression of ER stress response related proteins; GRP78, XBP1s, CHOP and ATF3 in monolayers (2D) or spheroids (3D) of HCC cell lines including SNU475 cells, SNU449 cells and Huh7 cells. (C-D) ASS1 mRNA levels by RT-PCR analysis in Huh7 cells and SNU475 cells with treatment of ER stress inducers; TG and TM. (E-F) ASS1 promoter activity by luciferase assay in Huh7 cells with treatment of TG and TM. ASS1 expression levels in Huh7 cells and SNU475 cells with treatment of (G) TG and (H) TM. (I) Immunofluorescence (IF) images showing ASS1 (green), ER (red), and nuclei (blue) in Huh7 cells after ER stress induction by TG and TM treatment. *P<0.05, **P<0.01 and ***P<0.001 compared to control group. TG;thapsigargin, TM;tunicamycin.

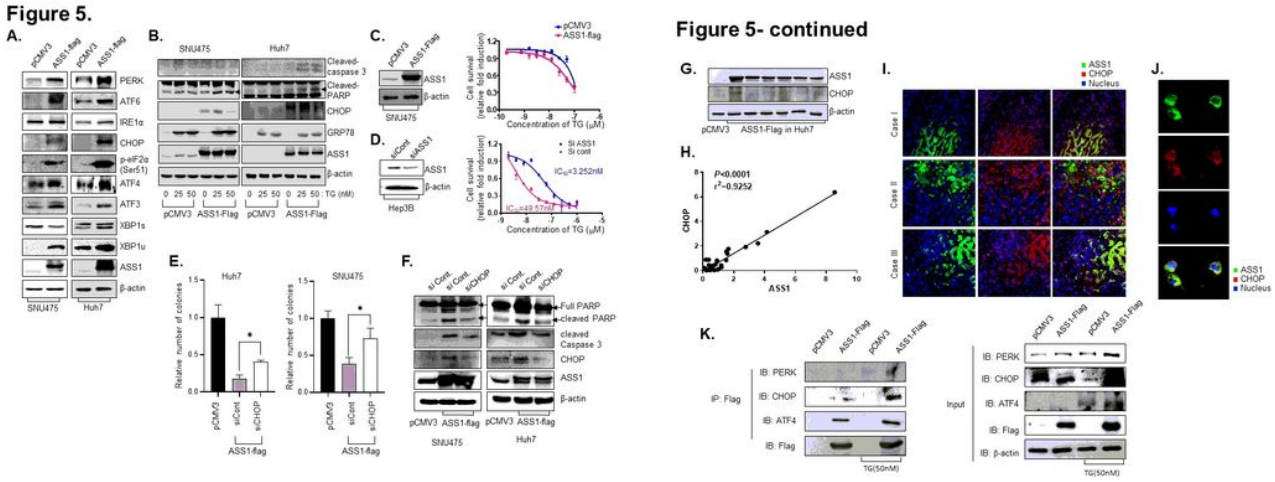

Figure 5

ASS1 controls cell fate through upregulation of CHOP in HCC (A) Expression of ER stress-related proteins; PERK, ATF6, IRE1a, CHOP, ATF3 XBP1s and XBP1u in pCMV3 or ASS1-flag-transfected Huh7 cells and SNU475 cells. (B) Expression of Apoptosis-related proteins; PARP and caspase 3 active forms and ER stress related proteins; CHOP and GRP78 in Huh7 cells and SNU475 cells after treatment with TG. Cell viability analysis of TG treatment in (C) pCMV3 or ASS1-flag transfected SNU475 cells and (D) siRNA against ASS1 transfected Hep3B cells. (E) The number of colony analysis and (F) the expression of apoptosis related proteins in Huh7 cells and SNU475 cells transfected with either non-specific control siRNA (siCont.) or CHOP siRNA (siCHOP) in ASS1 overexpressed Huh7 cells and SNU475 cells (G) Expression of ASS1 and CHOP in ASS1 overexpressed Huh7 cell transfected with non-specific siRNA (siCont.) or ASS1 siRNA (siASS1) by western blot assay. (H) The correlation expression levels between ASS1 and CHOP in tumor tissues from HCC patients. Immunofluorescence (IF) staining of ASS1 and CHOP in (I) tumor tissues from patients with liver cancer and (J) Huh7 cells. (K) Co-immunoprecipitation (IP) assay of Huh7 cells transfected with ASS1-Flag. The samples were analyzed by immunoblotting with an anti-PERK, ATF4, and CHOP. *P<0.05 compared to siControl group.

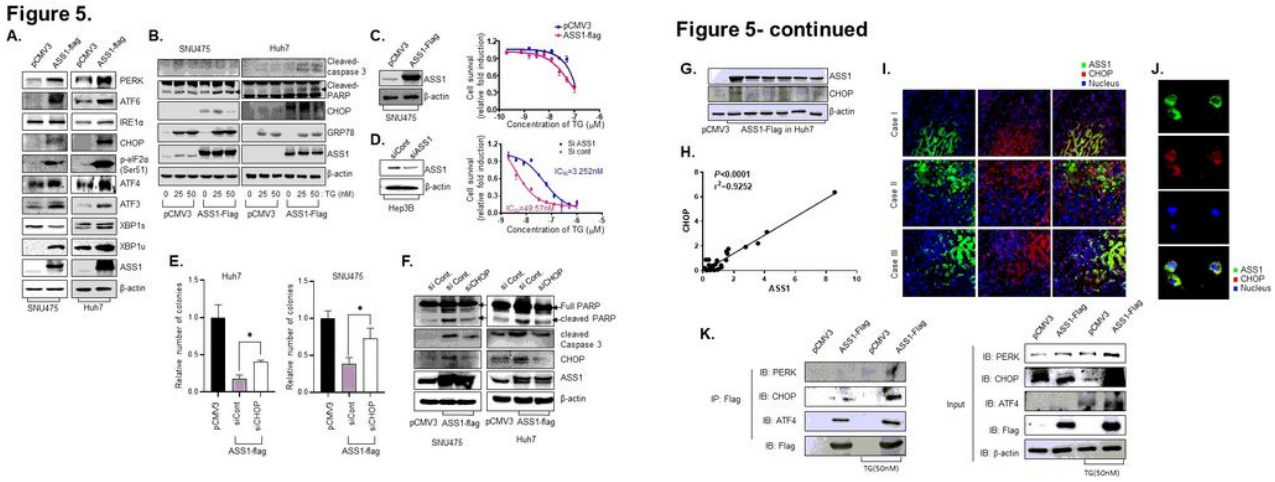

Figure 5

ASS1 controls cell fate through upregulation of CHOP in HCC (A) Expression of ER stress-related proteins; PERK, ATF6, IRE1a, CHOP, ATF3 XBP1s and XBP1u in pCMV3 or ASS1-flag-transfected Huh7 cells and SNU475 cells. (B) Expression of Apoptosis-related proteins; PARP and caspase 3 active forms and ER stress related proteins; CHOP and GRP78 in Huh7 cells and SNU475 cells after treatment with TG. Cell viability analysis of TG treatment in (C) pCMV3 or ASS1-flag transfected SNU475 cells and (D) siRNA against ASS1 transfected Hep3B cells. (E) The number of colony analysis and (F) the expression of apoptosis related proteins in Huh7 cells and SNU475 cells transfected with either non-specific control siRNA (siCont.) or CHOP siRNA (siCHOP) in ASS1 overexpressed Huh7 cells and SNU475 cells (G) Expression of ASS1 and CHOP in ASS1 overexpressed Huh7 cell transfected with non-specific siRNA (siCont.) or ASS1 siRNA (siASS1) by western blot assay. (H) The correlation expression levels between ASS1 and CHOP in tumor tissues from HCC patients. Immunofluorescence (IF) staining of ASS1 and CHOP in (I) tumor tissues from patients with liver cancer and (J) Huh7 cells. (K) Co-immunoprecipitation (IP) assay of Huh7 cells transfected with ASS1-Flag. The samples were analyzed by immunoblotting with an anti-PERK, ATF4, and CHOP. *P<0.05 compared to siControl group.

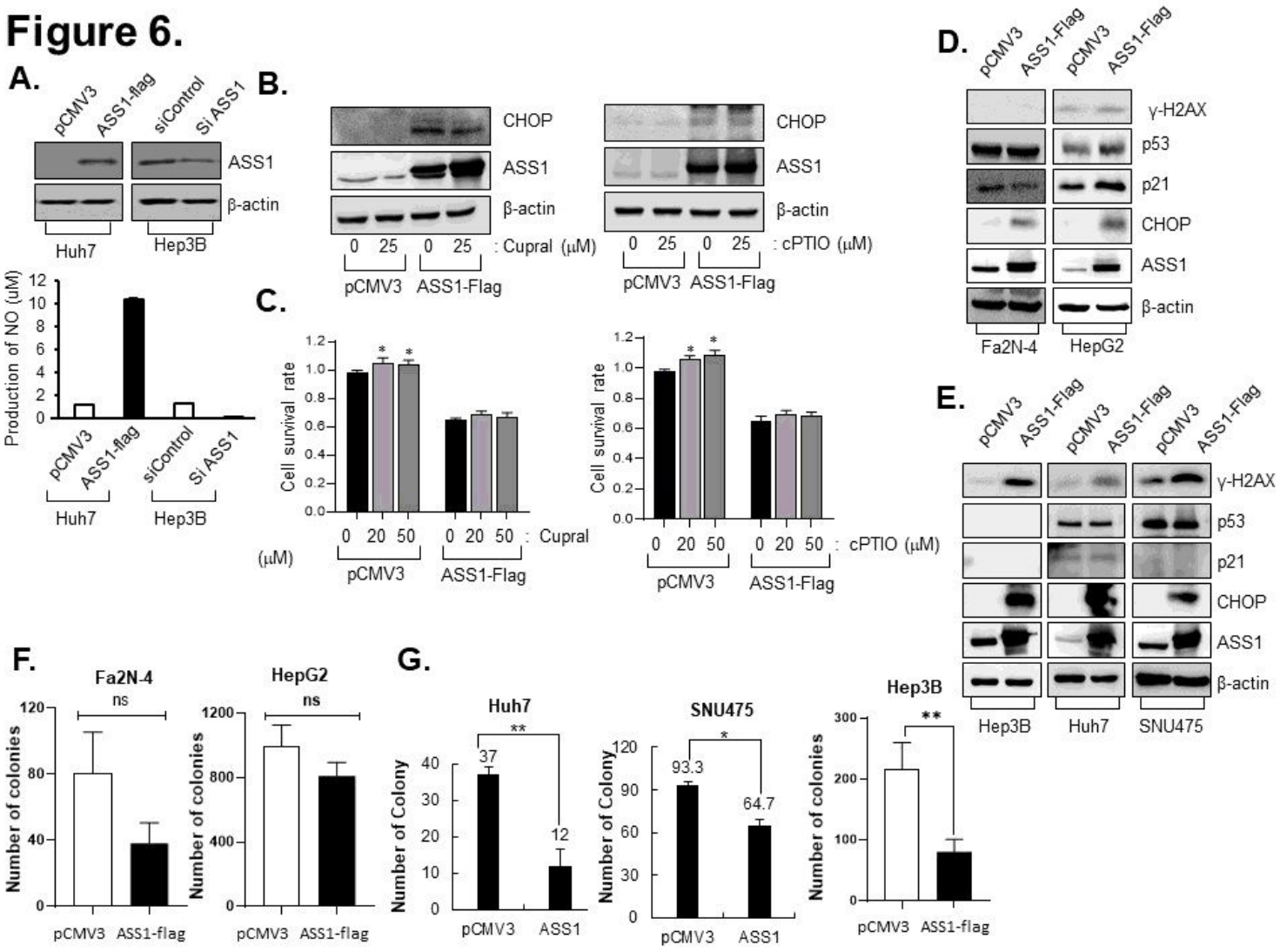

Figure 6

ASS1 acquires tumor suppressor activity independently of arginine metabolism and the p53 pathway (A) The NO production in ASS1-upregulation or downregulation in HCC cells. (B) ASS1 and CHOP expression levels and (C) cell survival analysis in pCMV3 or ASS1-treansfected Huh7 cells with the NO scavenger treatment; cupral (left panel) and cPTIO (right panel). (D) Phosphorylation of H2AX (γ-H2AX) and p53 pathway related proteins expression level in pCMV3- or ASS-flag transfected p53 wild type cells (Fa2N-4 and HepG2 cells) and (E) Colony formation assay in pCMV3- or ASS1-flag transfected p53-wild type. (F) Expression of γ-H2AX p53 related proteins in p53-null cell (Hep3B) and p53-mutant cells (Huh7 cells and SNU475 cells). (G) FFColony formation assay in pCMV3- or ASS1-flag transfected (G) p53-null and p53-mutant cells. *P<0.05, **P<0.01 compared to control group. ns; not significant, NO; nictic oxide

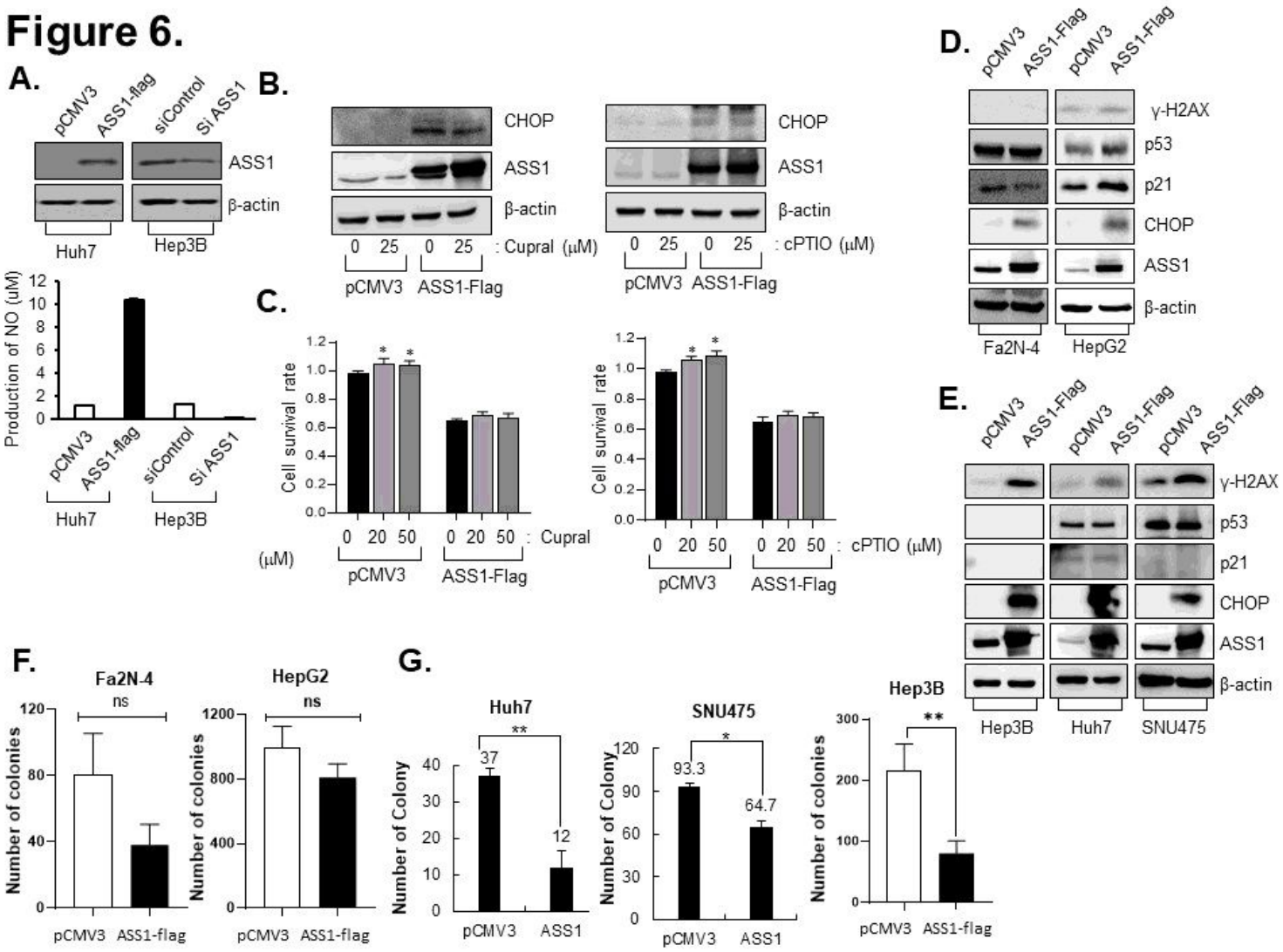

Figure 6

ASS1 acquires tumor suppressor activity independently of arginine metabolism and the p53 pathway (A) The NO production in ASS1-upregulation or downregulation in HCC cells. (B) ASS1 and CHOP expression levels and (C) cell survival analysis in pCMV3 or ASS1-treansfected Huh7 cells with the NO scavenger treatment; cupral (left panel) and cPTIO (right panel). (D) Phosphorylation of H2AX (γ-H2AX) and p53 pathway related proteins expression level in pCMV3- or ASS-flag transfected p53 wild type cells (Fa2N-4 and HepG2 cells) and (E) Colony formation assay in pCMV3- or ASS1-flag transfected p53-wild type. (F) Expression of γ-H2AX p53 related proteins in p53-null cell (Hep3B) and p53-mutant cells (Huh7 cells and SNU475 cells). (G) FFColony formation assay in pCMV3- or ASS1-flag transfected (G) p53-null and p53-mutant cells. *P<0.05, **P<0.01 compared to control group. ns; not significant, NO; nictic oxide

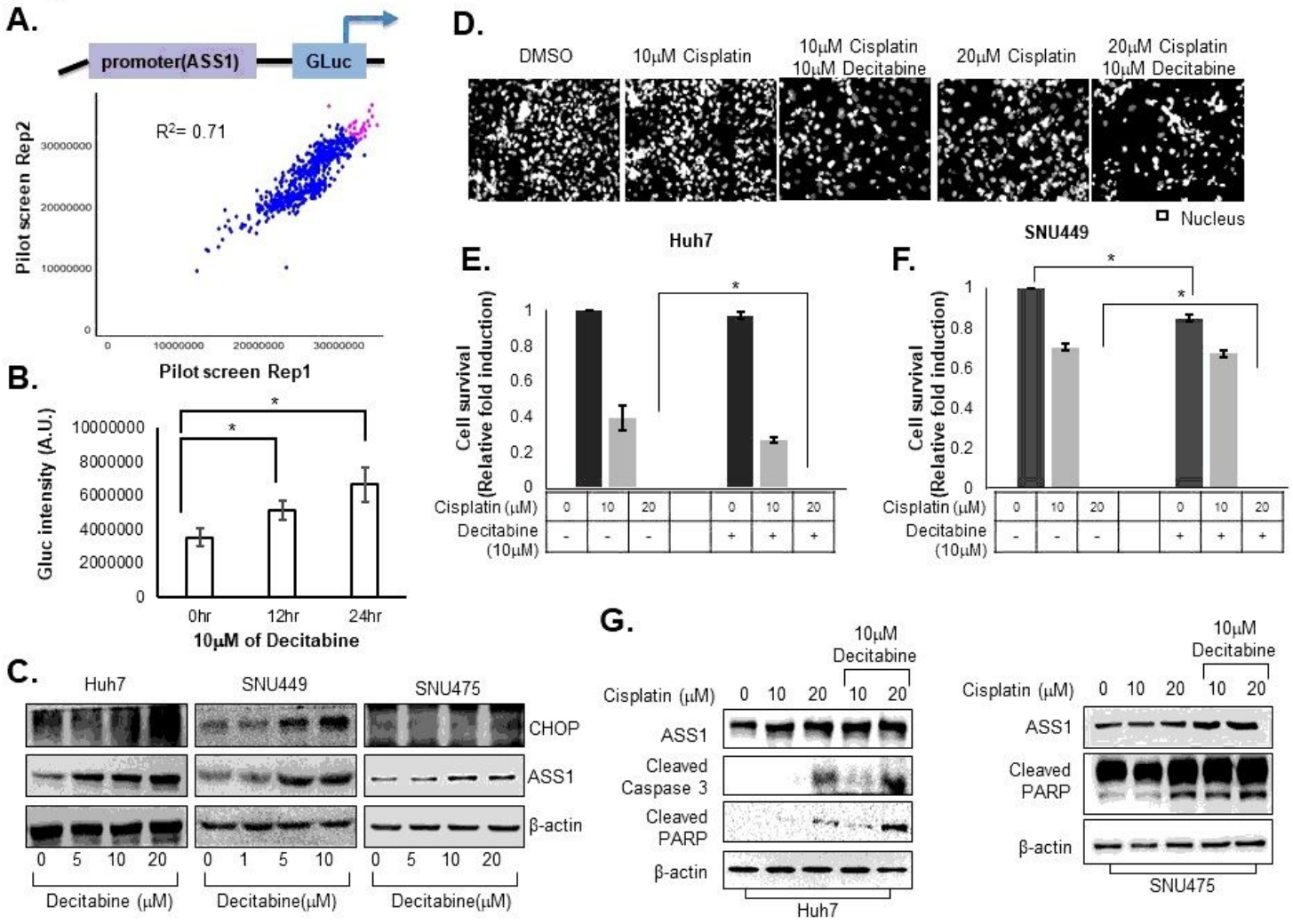

Figure 7

Decitabine improves efficacy of anti-HCC chemotherapeutic drugs by increasing ASS1 expression in HCC cells (A) the results of ASS1 promoter activity pilot screening. (B) ASS1 promoter activity in HEK293 cells treated with 10 μM decitabine for 12hr or 24hr by luciferase assay. (C) ASS1 and CHOP expression levels in Huh7 cells, SNU475 cells, and SNU449 cells treated with decitabine indicated concentration. (D) Representative of cell viability in Huh7 cells with combination treatment of cisplatin and decitabine. (E-F) Cell survival rates of Huh7 cells and SNU449 cells after combination treatment with 0, 10, or 20 μM cisplatin and 10 μM decitabine by nuclei counting. (G) Expression of apoptosis related proteins; cleaved caspase 3 and PARP activation form expression levels in Huh7 cells and SNU475 cells after combination treatment with 0, 10, or 20 μM cisplatin and 10 μM decitabine. *P<0.05 compared control group.

Figure 7.

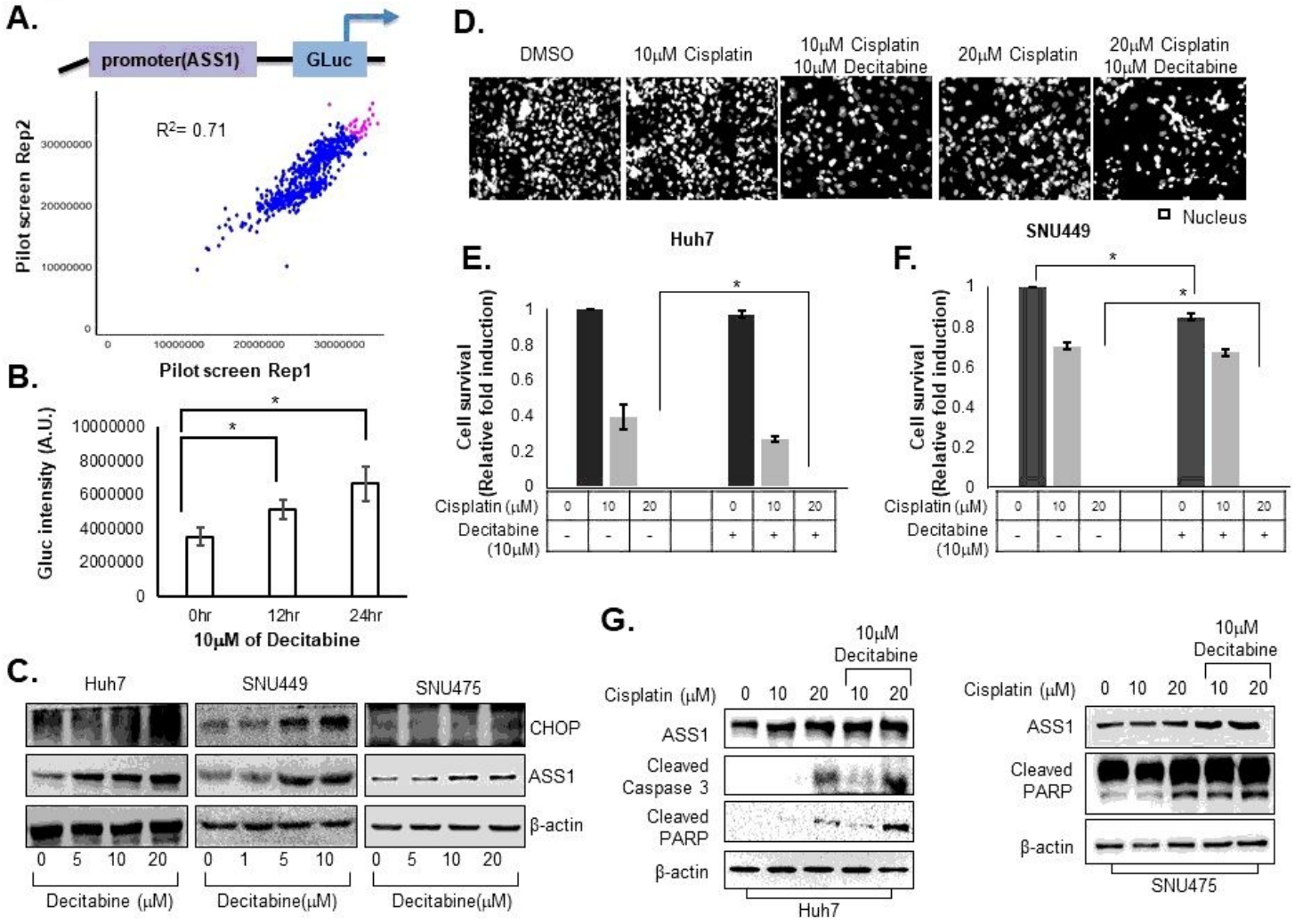

Figure 7

Decitabine improves efficacy of anti-HCC chemotherapeutic drugs by increasing ASS1 expression in HCC cells (A) the results of ASS1 promoter activity pilot screening. (B) ASS1 promoter activity in HEK293 cells treated with 10 μM decitabine for 12hr or 24hr by luciferase assay. (C) ASS1 and CHOP expression levels in Huh7 cells, SNU475 cells, and SNU449 cells treated with decitabine indicated concentration. (D) Representative of cell viability in Huh7 cells with combination treatment of cisplatin and decitabine. (E-F) Cell survival rates of Huh7 cells and SNU449 cells after combination treatment with 0, 10, or 20 μM cisplatin and 10 μM decitabine by nuclei counting. (G) Expression of apoptosis related proteins; cleaved caspase 3 and PARP activation form expression levels in Huh7 cells and SNU475 cells after combination treatment with 0, 10, or 20 μM cisplatin and 10 μM decitabine. *P<0.05 compared control group.

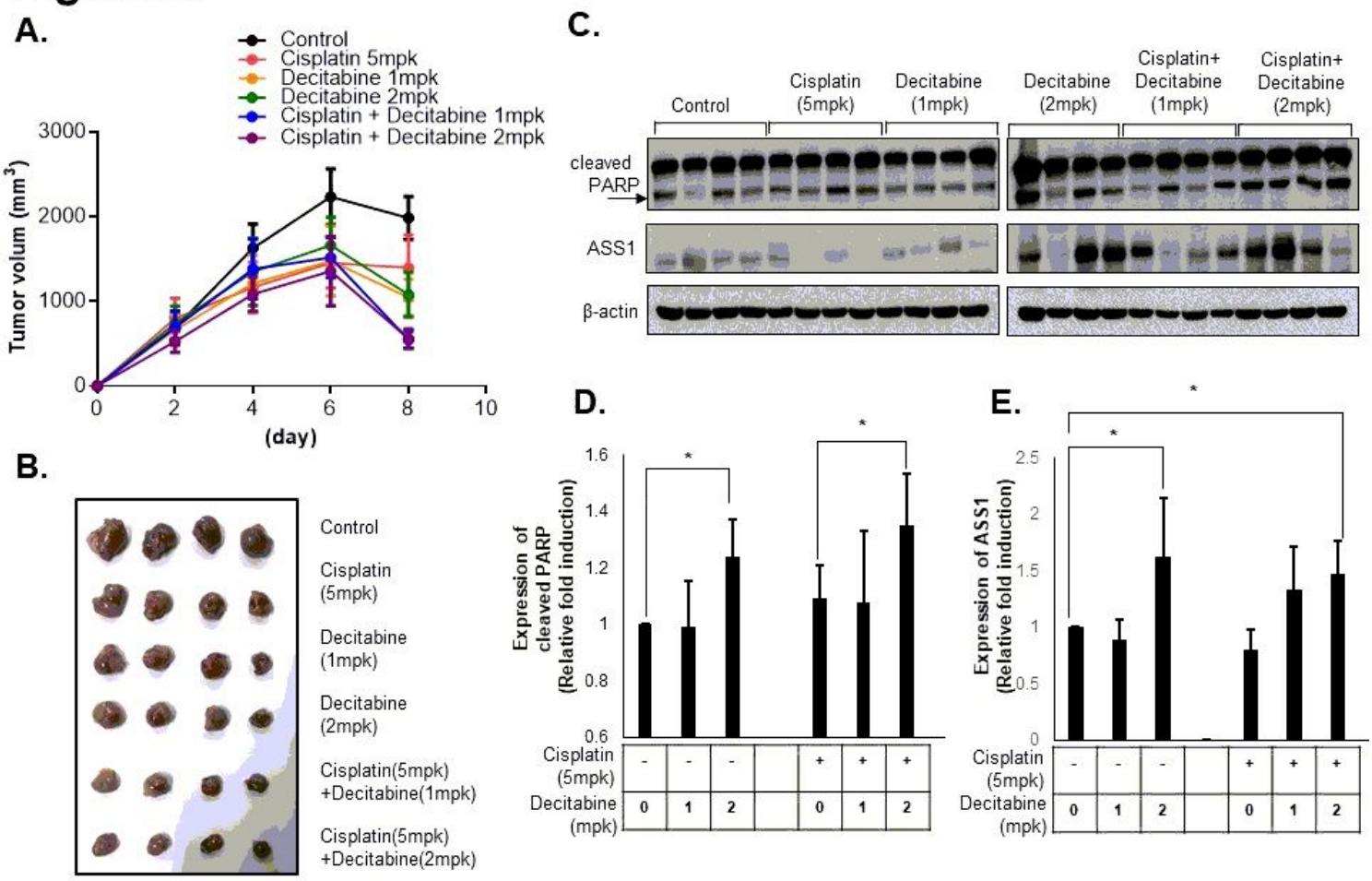

Figure 8

The combination treatment of cisplatin and decitabine improves efficacy of anti-HCC therapeutic in xenograft mice models (A) Tumor volume curves and (B) representative of tumors from xenograft mice treated with cisplatin (5 mpk) and decitabine (1 or 2mpk) (N=4). (C) PARP activation form (cleaved PARP) and ASS1 expression levels in tumor tissues of xenograft mice treated with cisplatin and decitabine by western blot assay. (D-E) Relative quantitative expression analysis of cleaved PARP and ASS1. *P<0.05 compared to control group.

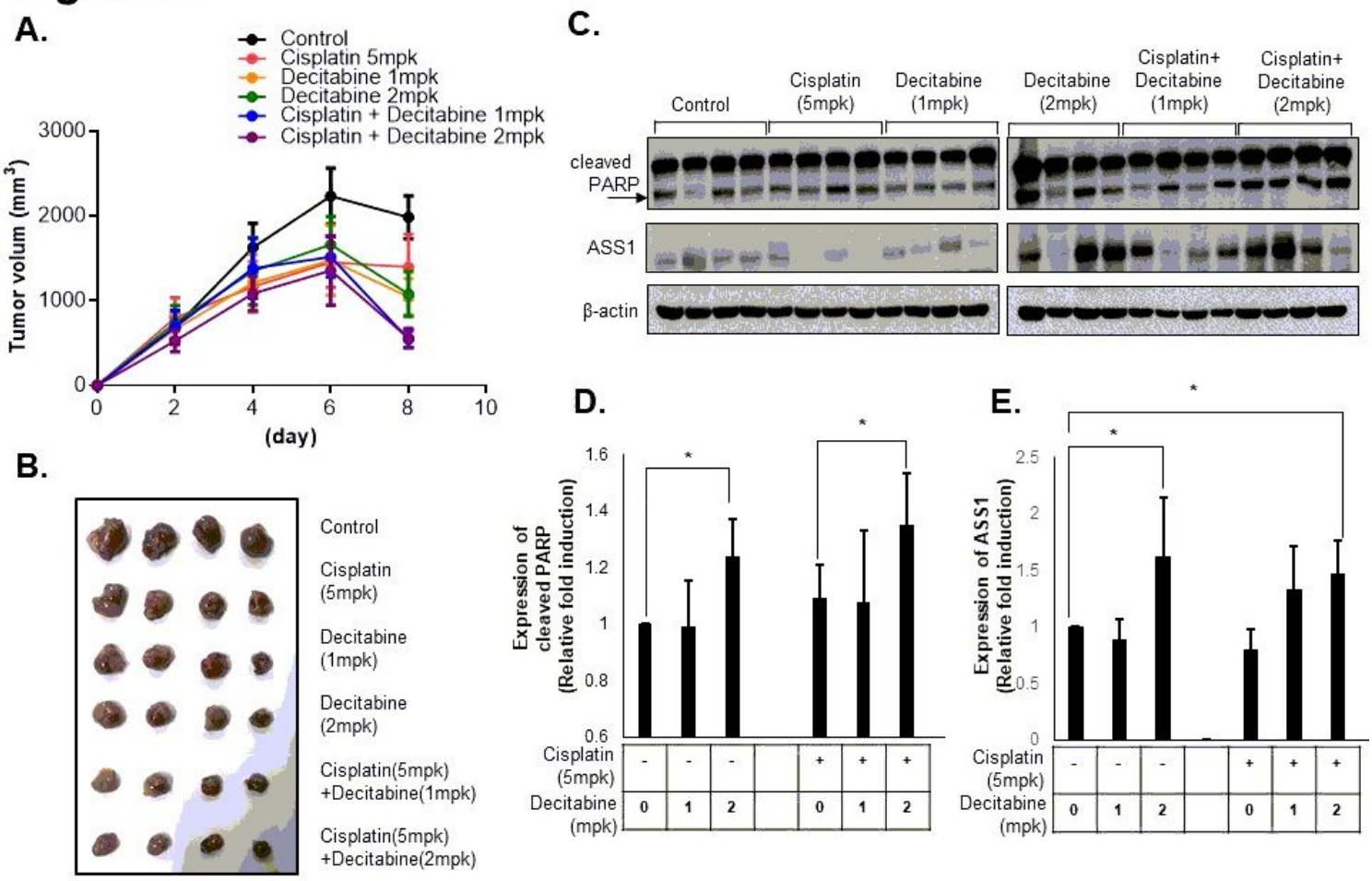

Figure 8

The combination treatment of cisplatin and decitabine improves efficacy of anti-HCC therapeutic in xenograft mice models (A) Tumor volume curves and (B) representative of tumors from xenograft mice treated with cisplatin (5 mpk) and decitabine (1 or 2mpk) (N=4). (C) PARP activation form (cleaved PARP) and ASS1 expression levels in tumor tissues of xenograft mice treated with cisplatin and decitabine by western blot assay. (D-E) Relative quantitative expression analysis of cleaved PARP and ASS1. *P<0.05 compared to control group.

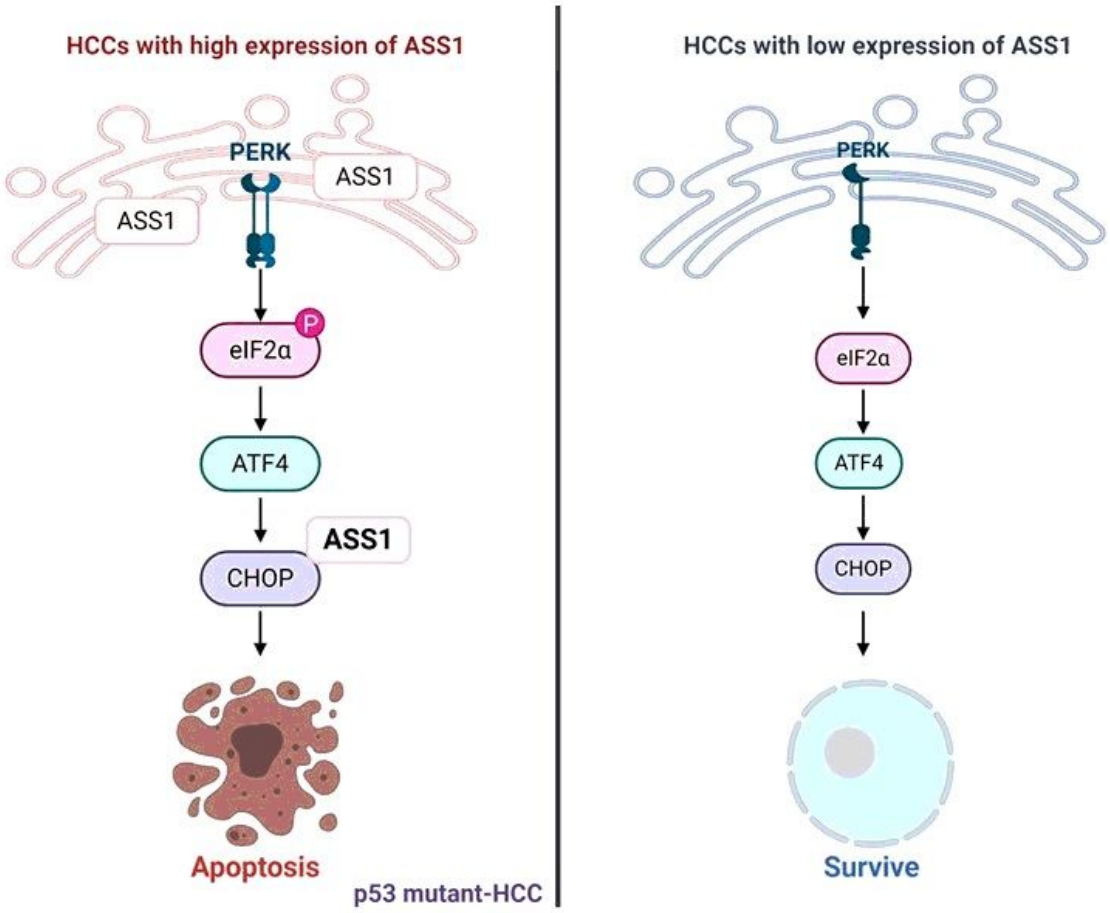

Figure 9

Graphical summary of novel functions of ASS1 as a tumor suppressor through ER stress-induced apoptosis in mutant p53 HCCs

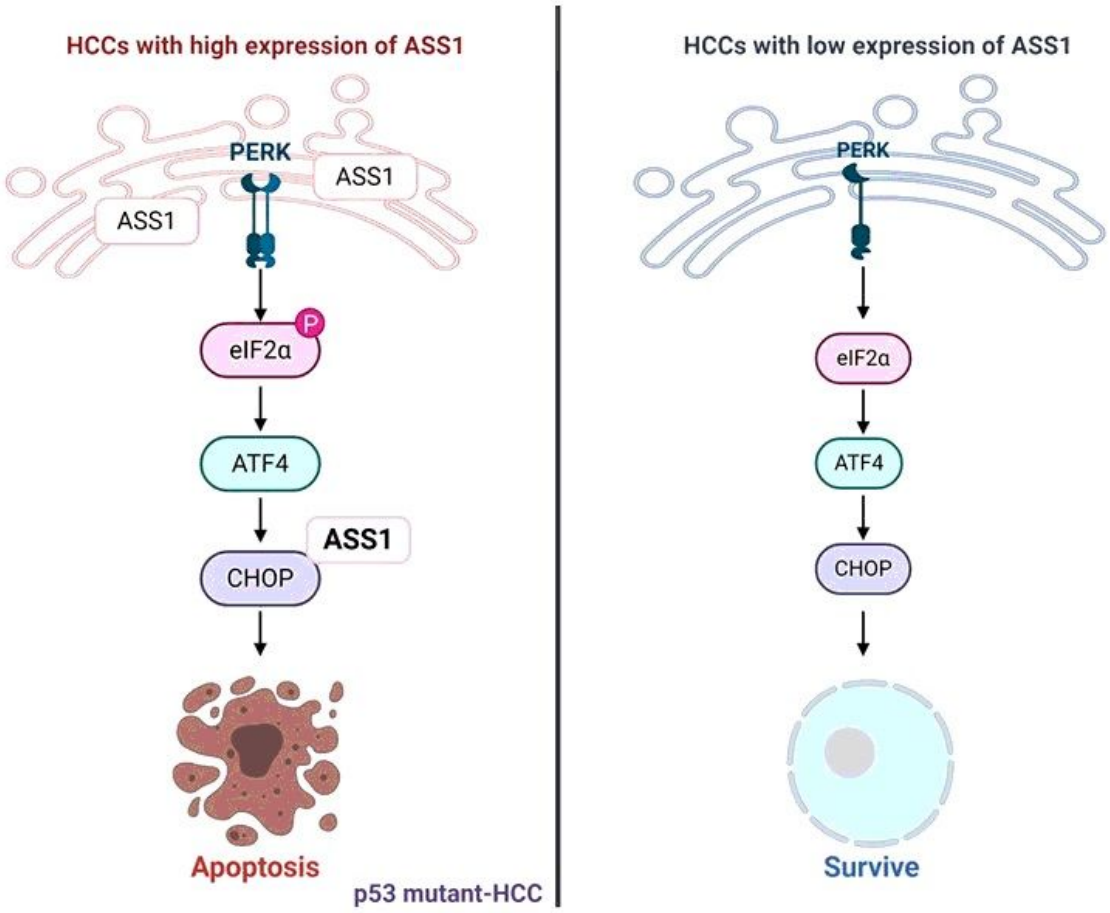

Figure 9

Graphical summary of novel functions of ASS1 as a tumor suppressor through ER stress-induced apoptosis in mutant p53 HCCs

Supplementary Files

This is a list of supplementary files associated with this preprint. Click to download.

- SupplementaryFiguresTables.pdf
- SupplementaryFiguresTables.pdf